Domestic Members
AmerenUE
Callaway
American Electric Power Co.
D.C. Cook 1 & 2
Arizona Public Service Co.
Palo Verde 1, 2 & 3
Constellation Energy Group
Calvert Cliffs 1 & 2
Dominion Nuclear Connecticut
Millstone 2 & 3
Dominion Virginia Power
North Anna 1 & 2
Surry 1 & 2
Duke Energy
Catawba 1 & 2
McGuire 1 & 2
Entergy Nuclear Northeast
Indian Point 2 & 3
Entergy Nuclear South
ANO 2
Waterford 3
Exelon Generation Company LLC
Braidwood 1 & 2
Byron 1 & 2
FirstEnergy Nuclear Operating Co.
Beaver Valley 1 & 2
FPL Group
St. Lucie 1 & 2
Seabrook
Turkey Point 3 & 4
Nuclear Management Co.
Kewaunee
Palisades
Point Beach 1 & 2
Prairie Island
Omaha Public Power District
Fort Calhoun
Pacific Gas & Electric Co.
Diablo Canyon 1 & 2
Progress Energy
H. B. Robinson 2
Shearon Harris
PSEG – Nuclear
Salem 1 & 2
Rochester Gas & Electric Co.
R. E. Ginna
South Carolina Electric & Gas Co.
V. C. Summer
Southern California Edison
SONGS 2 & 3
STP Nuclear Operating Co.
South Texas Project 1 & 2
Southern Nuclear Operating Co.
J. M. Farley 1 & 2
A. W. Vogtle 1 & 2
Tennessee Valley Authority
Sequoyah 1 & 2
Watts Bar 1
TXU Electric
Commanche Peak 1 & 2
Wolf Creek Nuclear Operating Corp.
Wolf Creek

International Members
Electrabel
Doel 1, 2, 4
Tihange 1 & 3
Electricité de France
Kansai Electric Power Co.
Mihama 1
Takahama 1
Ohi 1 & 2
Korea Hydro & Nuclear Power Co.
Kori 1 – 4
Ulchin 3 & 4
Yonggwang 1 - 5
British Energy plc
Sizewell B
NEK
Krško
Spanish Utilities
Asco 1 & 2
Vandellos 2
Almaraz 1 & 2
Ringhals AB
Ringhals 2 – 4
Taiwan Power Co.
Maanshan 1 & 2

July 30, 2004

WOG-04-389

WCAP-16083-NP, Rev. 0
Project No. 694

Document Control Desk
U. S. Nuclear Regulatory Commission
Washington, DC 20555-0001

Subject: Westinghouse Owners Group
Transmittal of WCAP-16083-NP, Rev. 0, "Benchmark Testing of the FERRET Code for Least Squares Evaluation of Light Water Reactor Dosimetry," May 2004 (MUHP-7550)

This letter transmits four copies of WCAP-16083-NP, Rev. 0, "Benchmark Testing of the FERRET Code for Least Squares Evaluation of Light Water Reactor Dosimetry", dated May 2004. The Westinghouse Owners Group (WOG) is submitting WCAP-16083-NP, Rev. 0 in accordance with the Nuclear Regulatory Commission (NRC) licensing topical report program for review and acceptance for referencing in licensing actions. The methodology will be used for the validation of the neutron exposure of reactor vessel beltline materials.

Consistent with the NRC Office of Nuclear Reactor Regulation, Office Instruction LIC-500, Revision 2, "Processing Request for Reviews of Topical Reports," the WOG will participate in a telephone conference with the NRC to discuss and obtain a mutual agreement on the review schedule milestones (issuance of Request(s) for Additional Information and the draft Safety Evaluation) for WCAP-16083-NP, Rev. 0. Also consistent with LIC-500, Revision 2, the WOG expects the NRC to issue an acceptance letter documenting the mutually agreed upon review schedule (and estimated review hours) within 45 days of the date of this letter. The WOG requests that the NRC complete their review and issue a Safety Evaluation for WCAP-16083-NP, Rev. 0 by June 2005.

The WOG hereby agrees to pay review fees associated with the NRC review of WCAP-16083-NP, Rev 0. Correspondence related to this transmittal and invoices associated with the review of WCAP-16083-NP, Rev. 0, should be addressed to:

Mr. Gordon Bischoff
Manager, Owners Group Program Management Office
Westinghouse Electric Company
Mail Stop ECE 5-16
P. O. Box 355
Pittsburgh, Pennsylvania 15230-0355

D048

July 30, 2004
WOG-04-389

If you require further information, please contact Mr. Jim Molkenthin in the Owners Group Program Management Office at (860) 731-6727.

Sincerely,

Steven M. DiTommaso for

Frederick P. "Ted" Schiffley, II
Chairman, Westinghouse Owners Group

Enclosure

cc: Steering Committee
Management Committee
Licensing Subcommittee
Materials Subcommittee
Project Management Office
G. Shukla, USNRC (1L, 2R) (via Federal Express)
S. Dembek, USNRC
J. D. Andrachek, Westinghouse
S. Anderson, Westinghouse
R. Llovet, Westinghouse

Westinghouse Non-Proprietary Class 3

WCAP-16083-NP
Revision 0

May 2004

Benchmark Testing of the FERRET Code for Least Squares Evaluation of Light Water Reactor Dosimetry

WESTINGHOUSE NON-PROPRIETARY CLASS 3

WCAP-16083-NP

Revision 0

Benchmark Testing of the FERRET Code for Least Squares Evaluation of Light Water Reactor Dosimetry

WOG Program: MUHP 7550

S. L. Anderson

May 2004

Westinghouse Electric Company LLC
Energy Systems
P.O. Box 355
Pittsburgh, PA 15230-0355

©2004 Westinghouse Electric Company LLC
All Rights Reserved

LEGAL NOTICE

This report was prepared by Westinghouse as an account of Work sponsored by the Westinghouse Owners Group (WOG). Neither the WOG, any member of the WOG, Westinghouse, nor any person acting on behalf of any of them:

(A) Makes any warranty or representation whatsoever, express or implied, (I) with respect to the use of any information, apparatus, method, process, or similar item disclosed in this report, including merchantability and fitness for a particular purpose, (II) that such use does not infringe on or interfere with privately owned rights, including any party's intellectual property, or (III) that this report is suitable to any user's circumstance; or

(B) Assumes responsibility for any damages or other liability whatsoever (including any consequential damages, even if the WOG or any WOG representative has been advised of the possibility of such damages) resulting from any selection or use of this report or any information, apparatus, method, process, or similar item disclosed in this report."

COPYRIGHT NOTICE

This report has been prepared by Westinghouse Electric Company LLC, for the members of the Westinghouse Owners Group. Information in this report is the property of and contains copyright information owned by Westinghouse Electric Company LLC and/or its subcontractors and suppliers. It is transmitted to you in confidence and trust, and you agree to treat this document and the information contained therein in strict accordance with the terms and conditions of the agreement under which it was provided to you.

As a participating member of this Westinghouse Owners Group task, you are permitted to make the number of copies of the information contained in this report which are necessary for your internal use in connection with your implementation of the report results for your plant(s), in your normal conduct of business. Should implementation of this report involve a third party, you are permitted to make the number of copies of the information contained in this report which are necessary for the third party's use in supporting your implementation at your plant(s) in your normal conduct of business if you have received the prior, written consent of Westinghouse Electric Company LLC to transmit this information to a third party or parties. All copies made by you must include the copyright notice in all instances.

TABLE OF CONTENTS

LIST OF TABLES

LIST OF FIGURES

1.0 INTRODUCTION

In the assessment of the state of embrittlement of Light Water Reactor (LWR) pressure vessels, an accurate evaluation of the neutron exposure of the materials comprising the beltline region of the vessel is required. This exposure evaluation must, in general, include assessments not only at locations of maximum exposure at the inner diameter of the vessel, but also as a function of axial, azimuthal, and radial location throughout the vessel wall.

In order to satisfy the requirements of 10CFR50, Appendices G and H[1] for the calculation of pressure/temperature limit curves for normal heatup and cooldown of the reactor coolant system, fast neutron exposure levels must be defined at depths within the vessel wall equal to 25 and 75 percent of the wall thickness for each of the materials comprising the beltline region. These locations are commonly referred to as the 1/4T and 3/4T positions in the vessel wall. The 1/4T exposure levels are also used in the determination of upper shelf fracture toughness as specified in 10CFR50, Appendix G. In the determination of the pressurized thermal shock reference temperature (RT_{PTS}) for comparison with the applicable screening criteria as defined in 10CFR50.61,[2] maximum neutron exposure levels experienced by each of the beltline materials are required. These maximum levels will occur at the vessel inner radius. Furthermore, in the event that a probabilistic fracture mechanics analysis of the pressure vessel is performed, a complete neutron exposure profile is required for the entire volume of the pressure vessel beltline.

Methods acceptable to the NRC staff for the determination of the neutron exposure of LWR pressure vessels are described in Regulatory Guide 1.190, "Calculational and Dosimetry Methods for Determining Pressure Vessel Neutron Fluence."[3] This Regulatory Guide requires that the exposure projections be completed with a calculation and that measurements be used to qualify the calculational methodology as well as to identify biases in the calculations and to provide reliable estimates of the uncertainties in the exposure projections. The guide also stipulates that, in the determination of potential biases and uncertainties, measurement to calculation (M/C) comparisons should include a suitably weighted average of individual M/C values that accounts for the spectral coverage of the sensor set and the uncertainties in the measurements, the dosimetry cross-sections, and the neutron energy spectrum.

The methodology described in this report is based on the application of benchmarked plant specific neutron transport calculations providing neutron exposure maps throughout the reactor geometry including the pressure vessel wall, as well as all in-vessel and/or ex-vessel measurement locations. Evaluation of the dosimetry from the in-vessel and/or ex-vessel irradiations is subsequently accomplished with a least squares analysis including both the calculation and measurement data to establish best estimates of exposure parameters with reduced uncertainties at the locations of the measurements. The results of the least squares evaluations are used to demonstrate consistency among the various measurements and the baseline calculation at all measurement points and to validate the calculated results within the pressure vessel wall.

The use of a least squares adjustment method to perform dosimetry evaluations represents a rigorous approach to weighting the spectral coverage of individual sensor measurements and to combining the uncertainties associated with the transport calculations, measured reaction rates, and dosimetry cross-sections. Further, the results of the least squares evaluations provide comparisons of the best estimates of exposure parameters of interest (Fluence [E > 1.0 MeV] and iron atom displacements [dpa]) with the corresponding calculated results before adjustment. It is these damage exposure parameters and their uncertainties rather than individual sensor reaction rates that are of the ultimate interest.

This approach is summarized in ASTM E 944-02, "Standard Guide for Application of Neutron Spectrum Adjustment Methods in Reactor Surveillance,"[4] which states the following:

> "Adjustment methods provide a means for combining the results of neutron transport calculations with neutron dosimetry measurements in order to obtain optimal estimates for neutron damage exposure parameters with assigned uncertainties. The inclusion of measurements reduces the uncertainties for these parameter values and provides a test for the consistency between measurements and calculations and between different measurements."

It is important to emphasize that the least squares adjustments described in this report are used to combine multiple foil sensor measurements and plant specific calculated neutron spectra to determine best estimate exposure parameters only at in-vessel and ex-vessel measurement locations. This approach allows for appropriate spectral weighting of the measurements obtained from the multiple foil sensor sets and provides a rigorous treatment of the various measurement and calculational uncertainties associated with the process. Thus, the application of the least squares procedure allows the validation of the transport calculations to be based on comparisons of the exposure parameters of interest such as $\phi(E > 1.0\ MeV)$ rather than on some combination of individual sensor M/C ratios.

In this application, the FERRET code[5,6] is used for the least squares analysis of the dosimetry data sets. That is, the FERRET code is used solely to determine the best estimate exposure at locations where calculations and measurements coincide. The relationship between the best estimate exposure at the measurement locations and that at the pressure vessel wall, where no measurements exist, is not addressed internal to the FERRET code. Rather, the results of the plant specific neutron transport calculations are relied on to relate the neutron exposure at the pressure vessel wall to that at the various measurement locations within the reactor downcomer and or the ex-vessel cavity. This is analogous to an approach where one might use spatial calculations throughout the reactor core coupled with measurements at the center of selected fuel assemblies to generate detailed core power distribution maps which include locations removed from the measurement positions.

This is in contrast to the more sophisticated LEPRICON code system[7] that performs simultaneous adjustments of the calculated neutron spectra at the various measurement locations, as well as at the pressure vessel wall in order to determine the best estimate exposure with associated uncertainties within the pressure vessel itself.

The purpose of this report is to describe the application of the FERRET code to the least squares analysis of typical LWR dosimetry sets irradiated at either in-vessel or ex-vessel locations and to summarize the testing of the FERRET approach in both benchmark and power reactor neutron fields. The results provided in this report are intended to validate the FERRET code and the least squares procedure for use in the analysis of LWR dosimetry.

2.0 DESCRIPTION OF THE LEAST SQUARES METHODOLOGY

2.1 BACKGROUND

Least squares adjustment methods provide the capability to combine measurement data with the results of neutron transport calculations to establish a best estimate neutron energy spectrum with associated uncertainties at the measurement locations. Best estimates for key exposure parameters such as neutron flux, $\phi(E > 1.0$ MeV), or iron atom displacement rate, dpa/s, along with their uncertainties are then easily obtained from the adjusted spectrum. The use of measurements in combination with detailed transport calculations results in a reduced uncertainty in the calculated spectrum and provides a method to identify any biases or inconsistencies that may exist in the baseline transport calculation or in the measured data.

The application of least squares adjustment methods in LWR dosimetry analysis is common throughout the dosimetry community. The American Society for Testing and Materials (ASTM) has addressed the use of adjustment codes in ASTM E944 "Application of Neutron Spectrum Adjustment Methods in Reactor Surveillance," and many industry workshops have been held to discuss the various applications. For example, the ASTM-EURATOM Symposia on Reactor Dosimetry holds workshops on neutron spectrum unfolding and adjustment techniques at each of its bi-annual conferences.

In ASTM E944, a comprehensive listing of available adjustment codes commonly employed in reactor surveillance programs including STAY'SL[8], LSL-M2[9], FERRET, and LEPRICON is provided. Each of these codes is publicly available from the Radiation Safety Information Computational Center (RSICC) at the Oak Ridge National Laboratory (ORNL).

The FERRET code was initially developed at the Hanford Engineering Development Laboratory (HEDL) and has had extensive use in both the Liquid Metal Fast Breeder (LMFBR) program and the NRC sponsored Light Water Reactor Surveillance Dosimetry Improvement Program (LWR-PV-SDIP). Examples of the prior use of the FERRET code for LWR applications include: 1) a re-evaluation of the dosimetry from commercial pressurized water reactor surveillance capsules[12] and 2) an evaluation of the dosimetry included in the PCA blind test experiments.[13] Both of these applications were completed in support of the LWR-PV-SDIP program.

The former evaluation was carried out to establish an updated surveillance capsule dosimetry data base for use in the establishment of improved trend curves defining the radiation induced shift in reference nil-ductility transition temperature and the drop in upper shelf energy versus neutron fluence or displacements per atom (dpa). These updated correlations were later used in the development of the trend curve data appearing in Regulatory Guide 1.99, Revision 2.[14, 15, 16, 17] The latter evaluation was completed to provide estimates of key exposure parameters (Fluence $E > 1.0$ MeV and dpa) for use in performing blind tests of neutron transport calculations in the PCA facility.[12, 13] This, in turn, allowed blind test comparisons of calculated exposure parameters directly with the least squares results in addition to the comparisons with measured reaction rates obtained from the multiple foil sensor sets included in the PCA irradiations.

As a result of participation in several cooperative efforts associated with the LWR-PV-SDIP, the FERRET approach was adopted by Westinghouse in the mid 1980's as the preferred approach to the evaluation of LWR surveillance dosimetry. The least squares methodology was judged to be superior to the previously employed spectrum averaged cross-section approach that is totally dependent on the accuracy of the shape of the calculated neutron spectrum at the measurement

locations. Further, the application of the least squares methodology allowed for a rigorous treatment of the uncertainties associated with the dosimetry evaluation process.

2.2 APPLICATION OF THE METHODOLOGY

In general, the least squares methods, as applied to LWR dosimetry evaluations, act to reconcile the measured sensor reaction rate data, dosimetry reaction cross-sections, and the calculated neutron energy spectrum within their respective uncertainties. For example,

$$R_i \pm \delta_{R_i} = \sum_g (\sigma_{ig} \pm \delta_{\sigma_{ig}})(\phi_g \pm \delta_{\phi_g})$$

relates a set of measured reaction rates, R_i, to a single neutron spectrum, ϕ_g, through the multigroup dosimeter reaction cross-section, σ_{ig}, each with an uncertainty δ. The primary objective of the least squares evaluation is to produce unbiased estimates of the neutron exposure parameters at the location of the measurement.

The application of the least squares methodology requires the following input:

1 - The calculated neutron energy spectrum and associated uncertainties at the measurement location.

2 - The measured reaction rates and associated uncertainty for each sensor contained in the multiple foil set.

3 - The energy dependent dosimetry reaction cross-sections and associated uncertainties for each sensor contained in the multiple foil sensor set.

For LWR dosimetry applications, the calculated neutron spectrum is obtained from the results of plant specific neutron transport calculations that follow the guidelines specified in Regulatory Guide 1.190.[3]

The sensor reaction rates are derived from the measured specific activities obtained using established ASTM procedures. The dosimetry reaction cross-sections and uncertainties are obtained from the SNLRML dosimetry cross-section library. Each of these critical input parameters and associated uncertainties are discussed in this section.

2.3 NEUTRON TRANSPORT CALCULATIONS AND UNCERTAINTIES

An accurate plant specific neutron transport solution with its associated uncertainty represents the foundation upon which the least squares analysis of in-vessel and ex-vessel dosimetry sets builds. Therefore, in this section, the methodology employed by Westinghouse to perform neutron and gamma ray transport calculations for LWR applications is described in some detail. Also, included is a discussion of the benchmarking of the analysis approach and the resultant uncertainties associated with the calculational results.

For most routine analyses, the calculation of the neutron and gamma ray environment within the reactor geometry is completed on a fuel cycle specific basis using the following three-dimensional flux synthesis technique:

$$\phi(r,\theta,z) = [\phi(r,\theta)] * [\phi(r,z)]/[\phi(r)]$$

where $\phi(r,\theta,z)$ is the synthesized three-dimensional neutron flux distribution, $\phi(r,\theta)$ is the transport solution in r,θ geometry, $\phi(r,z)$ is the two-dimensional solution for a cylindrical reactor model using the actual axial core power distribution, and $\phi(r)$ is the one-dimensional solution for a cylindrical reactor model using the same source per unit height as that used in the r,θ two-dimensional calculation.

All of the transport calculations are carried out using the DORT discrete ordinates code Version 3.1[10] and the BUGLE-96 cross-section library[11]. The BUGLE-96 library provides a 67 group coupled neutron-gamma ray cross-section data set produced specifically for light water reactor application. Anisotropic scattering is treated with a minimum P_3 legendre expansion and the angular discretization is modeled with a minimum S_8 order of angular quadrature. Energy and space dependent core power distributions as well as system operating temperatures are treated on a fuel cycle specific basis. The synthesis procedure combining the $\phi(r,\theta)$, $\phi(r,z)$, and $\phi(r)$ transport solutions into the three-dimensional flux/fluence maps within the reactor geometry is accomplished via post-processing of the scalar flux files generated as a part of the DORT output.

In some extreme cases were three-dimensional effects reduce the accuracy of the synthesis approach, a fully three-dimensional analytical approach may be used to perform the transport analysis. In these instances, the TORT[10] three-dimensional discrete ordinates code, included as a part of the DOORS 3.1 code package, may be used in either x,y,z or r,θ,z geometry to effect the three-dimensional solution. As in the case of the transport calculations used in the synthesis analysis, the TORT calculations use the BUGLE-96 cross-section library with a minimum P_3 scattering approximation and a minimum S_8 order of angular quadrature.

2.3.1 GEOMETRIC MODELING

In developing an analytical model of the reactor geometry of the LWR reactor geometry, nominal design dimensions are normally employed for the various structural components. In some cases as-built dimensions are available; and, in those instances, the more accurate as-built data are used for model development. However, for the most part as built dimensions of the components in the beltline region of the reactor are not available, thus, dictating the use of design dimensions. Likewise, water temperatures and, hence, coolant density in the reactor core and downcomer regions of the reactor are normally taken to be representative of full power operating conditions. The reactor core itself is treated as a homogeneous mixture of fuel, cladding, water, and miscellaneous core structures such as fuel assembly grids, guide tubes, etc. Sensitivities of the analytical results to tolerances in the internals dimensions, as well as to fluctuations in water temperature are discussed and quantified in Section 2.3.4.

The r,θ geometric mesh description of the reactor model is normally accomplished using from 150 to 250 radial intervals and 60 to 110 azimuthal intervals depending on the overall size of the reactor and on the complexity required to model the core periphery, the in-vessel surveillance capsules, and the details of the reactor cavity. Mesh sizes are chosen to assure that proper convergence of the inner iterations is achieved on a pointwise basis. The pointwise inner iteration flux convergence criterion utilized in the r,θ calculations is set at a value of 0.001.

The mesh selection process results in a smaller spatial mesh in regions exhibiting steep gradients, in material zones of high cross-section (Σ_t), and at material interfaces. In the modeling of

in-vessel surveillance capsules, a minimum set of 3 radial by 3 azimuthal mesh are employed within the test specimen array to assure that sufficient information is produced for use in the assessment of fluence gradients within the materials test specimens, as well as in the determination of gradient corrections for neutron sensors. Additional radial and azimuthal mesh are employed to model the capsule structure surrounding the materials test specimen array. In modeling the stainless steel baffle region at the periphery of the core, a relatively fine spatial mesh is required to adequately describe this rectilinear component in r,θ geometry. In performing this x,y to r,θ transition, care is taken to preserve both the thickness and volume of the steel region in order to accurately address the shielding effectiveness of the component.

It should be noted that, although the example cited in this section is based on an octant symmetric model, the method itself is generally applicable even when such r,θ symmetry does not exist. The only change in the approach would be the use of a larger geometric model in the calculation.

As in the case of the r,θ model, the r,z model is also based on the use of nominal design dimensions and full power coolant densities. In this case, the homogenous core region is treated as an equivalent cylinder with a volume equal to that of the active core zone. The stainless steel former plates located between the core baffle and core barrel regions are also explicitly included in the model. The r,z geometric mesh description of the reactor model normally consists of from 130 to 230 radial intervals and from 90 to 150 axial intervals depending on the size of the reactor. Again, spatial mesh sizes are chosen to assure that proper convergence of the inner iterations was achieved on a pointwise basis. The pointwise inner iteration flux convergence criterion utilized in the r,z calculations is also set at a value of 0.001.

The one-dimensional radial model used in the synthesis procedure consists of the same radial spatial mesh array included in the r,z model. Thus, radial synthesis factors are easily determined on a mesh wise basis throughout the entire geometry.

2.3.2 CORE SOURCE

The spatial variation of the neutron source is generally obtained from a burnup weighted average of the respective power distributions from individual fuel cycles. These spatial distributions include pinwise gradients for all fuel assemblies located at the periphery of the core and typically include a uniform or flat distribution for fuel assemblies interior to the core. The spatial component of the neutron source is transposed from x,y to r,θ geometry by overlaying the mesh schematic to be used in the transport calculation on the pin by pin array and then computing the appropriate relative source applicable to each r,θ interval.

The x,y to r,θ transposition is accomplished by first defining a fine r,θ mesh working array. The Δr and $\Delta\theta$ of the fine mesh are usually chosen so that there is at least a 10x10 array of fine mesh over the area of each fuel pin at the core periphery. The coordinates of the center of each fine mesh interval and its associated relative source strength are assigned to the fine mesh based on the pin that is coincident with the center of the fine mesh. In the limit as Δr and $\Delta\theta$ approach zero, this technique becomes an exact transformation.

Each space mesh in the r,θ transport geometry is checked to determine if it lies totally within the area of a particular fine r,θ working mesh. If it does, the relative source of that fine mesh is assigned to the transport space mesh. If, on the other hand, the transport space mesh covers a part of one or more fine mesh, then the relative source assigned to the transport mesh is determined by an area weighting process as follows:

$$P_m = \frac{\sum_i A_i P_i}{\sum_i A_i}$$

where: Pm = the relative source assigned to transport mesh m.
Ai =the area of fine working mesh i within transport mesh m.
Pi = the relative source within fine working mesh i.

The energy distribution of the source is determined by selecting a fuel burnup representative of conditions averaged over the irradiation period under consideration and an initial fuel assembly enrichment characteristic of the core designs used over the applicable period. From this average burnup, a fission split by isotope including ^{235}U, ^{238}U, ^{238}Pu, ^{239}Pu, ^{240}Pu, and ^{241}Pu is derived; and, from that fission split, composite values of energy release per fission, neutron yield per fission, and fission spectrum are determined. These composite values are then combined with the r,θ spatial distribution to produce the overall absolute neutron source for use in the transport calculations.

2.3.3 VALIDATION OF THE TRANSPORT CALCULATIONS

The transport methodology described in Sections 2.3.1 and 2.3.2 of this report is identical to that described in the NRC approved version of WCAP-14040, Revision 3, Methodology Used to Develop Cold Overpressure Mitigation System Setpoints and RCS Heatup and Cooldown Limit Curves.[26] The validation of the transport methodology is based on the guidance provided in Regulatory Guide 1.190. In particular, the validation consists of the the following stages:

1 - Comparisons of calculations with benchmark measurements from the Pool Critical Assembly (PCA) simulator at the Oak Ridge National Laboratory (ORNL).

2 - Comparisons of calculations with surveillance capsule and reactor cavity measurements from the H. B. Robinson power reactor benchmark experiment.

3 - An analytical sensitivity study addressing the uncertainty components resulting from important input parameters applicable to the plant specific transport calculations used in the exposure assessments.

4 - Comparisons of calculations with a measurement data base obtained from a large number of surveillance capsules withdrawn from a variety of pressurized water reactors.

At each subsequent application of the methodology, comparisons are made with plant specific dosimetry results to demonstrate that the plant specific transport calculations are consistent with the uncertainties derived from the methods qualification.

The first stage of the methods validation addresses the adequacy of basic transport calculation and dosimetry evaluation techniques and associated cross-sections. This phase, however, does not test the accuracy of commercial core neutron source calculations nor does it address uncertainties in operational or geometric variables that impact power reactor calculations. The second stage of the validation addresses uncertainties that are primarily methods related and would tend to apply

generically to all fast neutron exposure evaluations. The third stage of the validation identifies the potential uncertainties introduced into the overall evaluation due to calculational methods approximations as well as to a lack of knowledge relative to various plant specific parameters. The overall calculational uncertainty is established from the results of these three stages of the validation process.

The following summarizes the uncertainties determined from the results of the first three stages of the validation process:

PCA Benchmark Comparisons	3%
H. B. Robinson Benchmark Comparisons	3%
Analytical Sensitivity Studies	11%
Internals Dimensions	3%
Vessel Inner Radius	5%
Water Temperature	4%
Peripheral Assembly Source Strength	5%
Axial Power Distribution	5%
Peripheral Assembly Burnup	2%
Spatial Distribution of the Source	4%
Other Factors	5%

The category designated "Other Factors" is intended to attribute an additional uncertainty to other geometrical or operational variables that individually have an insignificant impact on the overall uncertainty, but collectively should be accounted for in the assessment..

The uncertainty components tabulated above represent percent uncertainty at the 1σ level. In the tabulation, the net uncertainty of 11% from the analytical sensitivity studies has been broken down into its individual components. When the four uncertainty values listed above (3%, 3%, 11%, and 5%) are combined in quadrature, the resultant overall 1σ calculational uncertainty is estimated to be 13%.

To date, the methodology described in Section 2.2.1 coupled with the BUGLE-96 cross-section library has been used in the evaluation of dosimetry sets from 82 surveillance capsules from 23 pressurized water reactors. These withdrawals consisted of 2-5 capsules from individual reactors. The comparisons of the plant specific calculations with the results of the capsule dosimetry are used to further validate the calculational methodology within the context of a 1σ calculational uncertainty of 13%.

2.3.4 UNCERTAINTY INPUT TO THE LEAST SQUARES ADJUSTMENT

The neutron spectrum input to the least squares adjustment procedure is obtained directly from the results of plant specific transport calculations for each sensor location. The spectrum at each location is input in an absolute sense (rather than as simply a relative spectral shape). Therefore, within the constraints of the assigned uncertainties, the calculated data are treated equally with the measurements. The input uncertainties associated with the calculated spectrum must be consistent with the benchmarking results discussed in Section 2.3.3.

The uncertainty matrix for the calculated spectrum is constructed from the following relationship:

$$M_{g'g} = R_n^2 + R_g * R_{g'} * P_{g'g}$$

where R_n specifies an overall fractional normalization uncertainty and the fractional uncertainties $R_{g'}$ and R_g specify additional random groupwise uncertainties that are correlated with a correlation matrix given by:

$$P_{g'g} = [1 - \vartheta] * \delta_{g'g} + \vartheta * e^{-H}$$

where

$$H = \frac{(g - g')^2}{2\gamma^2}$$

The first term in the correlation matrix equation specifies purely random uncertainties, while the second term describes the short range correlations over a group range γ (θ specifies the strength of the latter term). The value of δ is 1.0 when g = g' and 0.0 otherwise.

The normalization uncertainty pertains primarily to the magnitude of the spectrum, whereas, the groupwise uncertainties deal with the shape of the spectrum relative to energy.
A typical set of parameters defining the input uncertainties for the calculated spectrum is as follows:

Flux Normalization Uncertainty (Rn)	15%
Flux Group Uncertainties (Rg, Rg')	
(E > 0.0055 MeV)	15%
(0.68 eV < E < 0.0055 MeV)	29%
(E < 0.68 eV)	52%
Short Range Correlation (θ)	
(E > 0.0055 MeV)	0.9
(0.68 eV < E < 0.0055 MeV)	0.5
(E < 0.68 eV)	0.5
Flux Group Correlation Range (γ)	
(E > 0.0055 MeV)	6
(0.68 eV < E < 0.0055 MeV)	3
(E < 0.68 eV)	2

These uncertainty assignments provide an input covariance matrix are consistent with the calculational uncertainties defined through the benchmarking process.

2.4 REACTION RATE MEASUREMENTS AND UNCERTAINTIES

Measurements at operating power reactors are generally accomplished with comprehensive multiple foil sensor sets including radiometric monitors (RM) and, in some instances for ex-vessel monitoring, solid state track recorders (SSTR). In general, sensor sets employed in Westinghouse dosimetry programs include materials in which the following reactions can be measured:

In-Vessel	Ex-Vessel
$^{63}Cu(n,\alpha)^{60}Co$	$^{63}Cu(n,\alpha)^{60}Co$ (Cd Covered)
$^{46}Ti(n,p)^{46}Sc$	$^{46}Ti(n,p)^{46}Sc$ (Cd Covered)
$^{54}Fe(n,p)^{54}Mn$	$^{54}Fe(n,p)^{54}Mn$ (Cd Covered)
$^{58}Ni(n,p)^{58}Co$	$^{58}Ni(n,p)^{58}Co$ (Cd Covered)
$^{238}U(n,f)FP$ (Cd Covered)	$^{238}U(n,f)FP$ (Cd Covered)
$^{237}Np(n,f)FP$ (Cd Covered)	$^{237}Np(n,f)FP$ (Cd Covered)
$^{59}Co(n,\gamma)^{60}Co$	$^{59}Co(n,\gamma)^{60}Co$
$^{59}Co(n,\gamma)^{60}Co$ (Cd Covered)	$^{59}Co(n,\gamma)^{60}Co$ (Cd Covered)

These sensor sets provide adequate spectrum coverage in the fast neutron energy range above approximately 0.5 MeV and also include bare and cadmium covered cobalt sensors to provide an assessment of the thermal neutron flux at the measurement locations. These sensor sets are fully consistent with the guidance specified in Section 2.1.1 of Regulatory Guide 1.190. Similar sensor set designs are also utilized by other vendors of LWR dosimetry programs.

Following irradiation, the specific activity of each of the radiometric sensors is determined using the latest version of ASTM counting procedures for each reaction. In particular, the following standards are applicable to the radiometric sensors typically used in LWR programs:

E523 Standard Test Method for Measuring Fast Neutron Reaction Rates by Radioactivation of Copper.

E526 Standard Test Method for Measuring Fast Neutron Reaction Rates by Radioactivation of Titanium.

E263 Standard Test Method for Measuring Fast Neutron Reaction Rates by Radioactivation of Iron.

E264 Standard Test Method for Measuring Fast Neutron Reaction Rates by Radioactivation of Nickel.

E704 Standard Test Method for Measuring Fast Neutron Reaction Rates by Radioactivation of Uranium-238.

E705 Standard Test Method for Measuring Fast Neutron Reaction Rates by Radioactivation of Neptunium-237.

E481 Standard Test Method for Measuring Neutron Fluence Rate by Radioactivation of Cobalt and Silver.

E1005 Standard Method for Application and Analysis of Radiometric Monitors for Reactor vessel Surveillance.

E481 Standard General Methods for Detector Calibration and Analysis of Radionuclides.

Following sample preparation and weighing, the specific activity of each sensor is determined using a germanium gamma spectrometer. In the case of multiple foil sensor sets, these analyses are usually completed by direct counting of each of the individual sensors, or, as is sometimes the case with ^{238}U and ^{237}Np fission monitors from in-vessel irradiations, by direct counting preceded by dissolution and chemical separation of cesium from the sensor.

For ex-vessel dosimetry irradiations, gradient chains or wires are often included with the multiple foil sensor sets. For these gradient measurements, individual sensors are obtained by cutting the chains into a series of segments to provide data at appropriate intervals over the extent of the beltline region of the pressure vessel. The determination of sensor specific activities in these segments then proceeds in the same fashion as for individual foils from the multiple foil sensor sets. In general, data from the following reactions are obtained from the gradient chain measurements.

$$^{54}Fe(n,p)^{54}Mn$$
$$^{58}Ni(n,p)^{58}Co$$
$$^{59}Co(n,\gamma)^{60}Co$$

These data can be used in conjunction with high purity foil measurements to provide mappings of the neutron environment external to the reactor pressure vessel.

Solid state track recorders (SSTR) have also been used for the measurement of fission reaction rates at ex-vessel dosimetry locations. The determination of reaction rates from these sensors is performed in accordance with the following ASTM standard:

E854 Standard test Method for Application and Analysis of Solid State Track Recorder (SSTR) Monitors for reactor Surveillance

In the SSTR analysis, the individual track recorders are optically scanned to determine the total number of fissions that occurred during the course of the irradiation. Since the scanning procedure results in an integral quantity representative of the entire irradiation, no radioactive decay corrections are required to determine the sensor reaction rates.

The individual radiometric and SSTR measurement data obtained from the counting laboratories, the physical characteristics of the sensors, and the operating history of the reactor are used to determine full power reaction rates characteristic of the irradiation period experienced by the foil sets. Generally, the reactor operating history data are obtained on a monthly basis for the sensor irradiation period. For the sensor sets used in both in-vessel and ex-vessel monitoring, the half-lives of the product isotopes are long enough that a monthly histogram describing reactor operation has proven to be an adequate representation for use in radioactive decay corrections.

For the radiometric sensors used in LWR irradiations, reaction rates referenced to full power operation are determined from the following equation:

$$R = \frac{A}{N_o F Y \sum_{j=1}^{n} \frac{P_j}{P_{max}} C_j (1 - e^{-\lambda t_j}) e^{\lambda t_d}}$$

where:

- A =measured specific activity (dps/g).
- R =sensor reaction rate averaged over the irradiation period and referenced to operation at a core power level of P_{ref} (rps/atom).
- N_0 =number of target element atoms per gram of sensor (atom/g).
- F =weight fraction of the target isotope in the target material.
- Y =number of product atoms produced per reaction.
- P_j =average core power level during irradiation period j (MW).
- P_{ref} =maximum or reference core power level of the reactor (MW).
- C_j =calculated ratio of $\phi(E > 1.0\ MeV)$ during irradiation period j to the time weighted average $\phi(E > 1.0\ MeV)$ over the entire irradiation period.
- λ =decay constant of the product isotope (s^{-1}).
- t_j =length of irradiation period j (s).
- t_d =decay time following irradiation period j (s).

and the summation is carried out over the total number of monthly intervals comprising the irradiation period.

In the above equation, the ratio P_j/P_{ref} accounts for month by month variation of power level within a given fuel cycle. The ratio C_j is calculated for each fuel cycle using the neutron transport methodology described in Section 2.1 of this report and accounts for the change in sensor reaction rates caused by variations in flux level due to changes in core power spatial distributions from fuel cycle to fuel cycle. For a single cycle irradiation, $C_j = 1.0$. However, for multiple fuel cycle irradiations, particularly those using low leakage fuel management, the additional C_j correction must be utilized. This additional correction can be quite significant for sensor sets that have been irradiated for many fuel cycles in a reactor that has transitioned from non-low leakage to low leakage fuel management.

Since SSTR sensors are integrating devices not susceptible to radioactive decay of a product isotope, measurements of fissions per target atom, A, are converted directly to reaction rates using the following equation:

$$R = \frac{A}{\sum \frac{P_j * t_j}{P_{ref}}}$$

where the denominator in the above equation represents the total effective full power seconds (EFPS) of reactor operation during the irradiation period of the solid state track recorders.

Prior to using the measured reaction rates for direct comparison with the results of transport calculations or as input to the least squares adjustment procedure, additional corrections must be made to ^{238}U measurements to account for the presence of ^{235}U impurities in the sensors and for the build-in of plutonium isotopes over the course of the irradiation. These corrections are location and fluence dependent and are obtained from a combination of calculated data from the

plant specific discrete ordinates analysis described in Section 2.1 of this report and, when available, measurements made with ^{235}U foils or solid state track recorders.

In addition to the corrections for competing neutron induced reactions in the ^{238}U sensors, corrections must also be made to both the ^{238}U and ^{237}Np sensor reaction rates to account for gamma-ray induced fission reactions that occur during the irradiation. These photo-fission corrections are also location dependent and are obtained from the transport calculational methodology discussed in Section 2.1.

Typical corrections to the measured fission rates at in-vessel and ex-vessel sensor locations are summarized as follows:

	Typical Correction	
	In-Vessel	Ex-Vessel
^{235}U Impurities	8-12%	0-15%
Pu Build-In	7-20%	<1%
$^{238}U(\gamma,f)$	4-6%	3-5%
$^{237}Np(\gamma,f)$	1-2%	<1%

It should be noted that the corrections listed are typical values for a PWR plant with in-vessel capsules mounted on the outer radius of the thermal shield. These values can not be used with a plant specific sensor set. Rather, the appropriate corrections must be determined for each sensor set based on the actual plant specific geometry and irradiation history.

Along with the reaction rates themselves, the uncertainty associated with each of these measurements is also an important input to the least squares adjustment procedure. The overall uncertainty in the measured reaction rates includes components due to the basic measurement process, the irradiation history corrections, and the corrections for competing reactions. A high level of accuracy in the reaction rate determinations is assured by using laboratory procedures that conform to the ASTM National Consensus Standards listed earlier in this Section. In all cases, the latest available versions of the applicable standards are used in the dosimetry evaluations.

From these standards, it is noted that the achievable uncertainties in the measured specific activities of each of the sensors comprising typical LWR multiple foil sensor sets are as follows:

Reaction	Precision	Bias
$^{63}Cu(n,\alpha)^{60}Co$	1%	3%
$^{46}Ti(n,p)^{46}Sc$	1%	3%
$^{54}Fe(n,p)^{54}Mn$	1%	3%
$^{58}Ni(n,p)^{58}Co$	1%	3%
$^{238}U(n,f)FP$	1%	5%
$^{237}Np(n,f)FP$	1%	5%
$^{59}Co(n,\gamma)^{60}Co$	1%	5%

These uncertainties included the effects of counting statistics, sample weighing, detector calibration, source/detector geometry corrections, and product nuclide branching ratios.

In determining reaction rates from the measured specific activities, the following additional uncertainties are incurred:

Reaction	Fission Yield	Product Half-Life	Competing Reactions
$^{63}Cu(n,\alpha)^{60}Co$		0.02%	
$^{46}Ti(n,p)^{46}Sc$		0.2%	
$^{54}Fe(n,p)^{54}Mn$		0.2%	
$^{58}Ni(n,p)^{58}Co$		0.2%	
$^{238}U(n,f)FP$	1%	0.1%	4%
$^{237}Np(n,f)FP$	2%	0.1%	1%
$^{59}Co(n,\gamma)^{60}Co$		0.02%	

After combing all of these uncertainty components, the sensor reaction rates derived from the counting and data evaluation procedures typically result in the following net uncertainties associated with the sensor reaction rates that are input to the least squares evaluation:

Reaction	Reaction Rate Uncertainty (1σ)
$^{63}Cu(n,\alpha)^{60}Co$	5%
$^{46}Ti(n,p)^{46}Sc$	5%
$^{54}Fe(n,p)^{54}Mn$	5%
$^{58}Ni(n,p)^{58}Co$	5%
$^{238}U(n,f)FP$	10%
$^{237}Np(n,f)FP$	10%
$^{59}Co(n,\gamma)^{60}Co$	5%

In addition to the adherence to ASTM National Consensus Standards in the evaluation of sensor reaction rates, the procedures used by Westinghouse have been periodically tested via round robin counting exercises included as part of the NRC sponsored Light Water Reactor Surveillance Dosimetry Improvement Program (LWR_SDIP) as well as by evaluation of fluence counting standards provided by the National Institute of Science and Technology (NIST). A summary of the results of these counting validations is as follows:

1980 Round robin counting of the foil sets irradiated at the Thermal Shield Back (TSB) and Pressure Vessel Face (PVF) positions of the PCA simulator.

1981 Round robin counting of additional foil sets included in the first metallurgical simulated surveillance capsule, also irradiated in the PCA benchmark mockup.

These two counting exercises involved direct comparisons with measurements obtained by the Hanford Engineering Development Laboratory (HEDL). At the time of these irradiations, HEDL was a prime contractor providing measurement services for the PCA benchmark and was cross calibrated with NIST and the MOL laboratory in Belgium.

1985 Counting and evaluation of $^{46}Ti(n,p)^{46}Sc$, $^{54}Fe(n,p)^{54}Mn$, and $^{58}Ni(n,p)^{58}Co$ certified fluence standards supplied by NIST.

Comparisons with fluence standards involve the determination not only of the reaction rate of each foil, but also of the spectrum averaged cross-section in the NIST ^{235}U irradiation facility. Thus, the comparisons with certified fluence standards test both the measurement process and the energy dependent reaction cross-sections used in the evaluation.

1992 Counting of NIST foils irradiated in an ex-vessel dosimetry experiment at the Trojan power reactor.

This exercise involved duplicate counting of a subset of irradiated foils by both Westinghouse and NIST to assure adequate cross-calibration of the laboratories so that data could be confidently mixed in the overall fluence evaluations performed by NIST and the Oak Ridge National Laboratory (ORNL).

1998 Round robin counting of ^{238}U and ^{237}Np certified fluence standards irradiated by NIST in the MDRF facility at the University of Michigan.

As in the case of the 1985 radiometric sensor evaluations, the fluence standard involved the determination of the reaction rate of each sensor, but also of the spectrum averaged cross-sections in the MDRF facility.

The results obtained from these counting comparisons are summarized as follows:

	[West]/[HEDL]		[West]/[NIST]			
	1980	1981	1985	1992	1995	Average
$^{63}Cu(n,\alpha)^{60}Co$	1.041	1.018		0.969		1.009
$^{46}Ti(n,p)^{46}Sc$	1.036		1.012	1.030		1.026
$^{54}Fe(n,p)^{54}Mn$	1.006	1.008	1.011	1.056		1.020
$^{58}Ni(n,p)^{58}Co$	1.006	0.990	1.028	1.029		1.013
$^{238}U(n,f)FP$	1.014	1.014			1.017	1.015
$^{237}Np(n,f)FP$	1.006	1.017			1.097	1.040
$^{59}Co(n,\gamma)^{60}Co$	1.017	1.017				1.017

These comparisons demonstrate that the procedures used by Westinghouse in the determination of sensor reaction rates have produced accurate and stable results over an extended period of time. The cross-comparisons with HEDL and NIST support the reaction rate uncertainties used by Westinghouse in performing LWR fluence evaluations.

In addition to these periodic comparisons, laboratory calibrations with NIST supplied sources are also carried out on a routine basis.

2.5 DOSIMETRY CROSS-SECTIONS AND UNCERTAINTIES

The third key set of input data for the least squares procedure includes the reaction cross-sections for each of the sensors included in the multiple foil dosimetry packages. The reaction rate cross-sections used by Westinghouse are taken from the SNLRML library.[23] This data library provides reaction cross-sections and associated uncertainties, including covariances, for 66 dosimetry sensors in common use. Both the cross-sections and the uncertainties are provided in a fine multi-group structure for use in least squares adjustment applications.

These cross-sections were compiled from the most recent cross-section evaluations including ENDF/B-VI and IRDF-90[24] and have been tested with respect to their accuracy and consistency for least squares analyses. Further, the library has been empirically tested for use in fission spectra determination as well as in the fluence and energy characterization of 14 MeV neutron sources. Detailed discussions of the contents of the SNLRML library along with the evaluation process for each of the sensors is provided in Reference 23.

For the sensors of interest to LWR dosimetry applications, the following uncertainties in the fission spectrum averaged cross-sections are provided in the SNLRML documentation package:

Reaction	Uncertainty (1σ)
$^{63}Cu(n,\alpha)^{60}Co$	4.08-4.16%
$^{46}Ti(n,p)^{46}Sc$	4.51-4.87%
$^{54}Fe(n,p)^{54}Mn$	3.05-3.11%
$^{58}Ni(n,p)^{58}Co$	4.49-4.56%
$^{238}U(n,f)FP$	0.54-0.64%
$^{237}Np(n,f)FP$	10.32-10.97%
$^{59}Co(n,\gamma)^{60}Co$	0.79-3.59%

These tabulated ranges provide an indication of the dosimetry cross-section uncertainties associated with typical sensor sets used in LWR irradiations.

3.0 TESTING OF THE FERRET PROCESSING PROCEDURES

As noted in Section 2.0 of this report, the FERRET least squares adjustment code is employed by Westinghouse to combine the results of plant specific neutron transport calculations, dosimetry reaction cross-sections, and multiple foil reaction rate measurements to determine the best estimate values of damage exposure parameters (fluence [E > 1.0 MeV] and iron atom displacements [dpa]) along with their associated uncertainties at the measurement location.

As implemented in the FERRET analysis, the least squares evaluation of a given data set can be subdivided into the following two stages:

1 - A pre-adjustment procedure performed by the SAND module that processes the calculated neutron spectrum and the SNLRML dosimetry cross-sections into the 53 energy group structure required by the FERRET module.

2 - The subsequent application of the least squares algorithm in the FERRET module itself.

These two stages of the overall least squares adjustment procedure were individually tested by data comparisons in standard and benchmark fields as well as by analysis of a series of in-vessel and ex-vessel irradiations at operating power reactors.

In this section, results of least squares evaluations of dosimetry results from irradiations in the National Institute of Standards and Technology (NIST) Standard ^{235}U thermal fission field, the NIST Standard ^{252}Cf spontaneous fission field, the PCA simulator benchmark, and the H. B. Robinson power reactor benchmark are presented and discussed. In addition, results of the least squares evaluation of a database of in-vessel and ex-vessel power reactor measurements are described. These power reactor evaluations include data from a variety of different reactor designs and for several repeat measurement campaigns at individual reactors.

3.1 DATA COMPARISONS IN THE NIST ^{235}U FISSION FIELD

The sensor reaction cross-sections and associated uncertainties play a key role in the least squares evaluation of dosimetry data sets. Therefore, it is important to assess both the overall accuracy of these cross-sections and the impact on that accuracy of any data processing included in the evaluation procedure.

The least squares approach used by Westinghouse makes use of the SNLRML dosimetry cross-section library. This comprehensive library has been recommended in ASTM E1018-01, "Standard Guide for Application of ASTM Evaluated Cross-Section Data File"[18] for use in LWR applications. The library is provided by the Radiation Safety Information Computational Center (RSICC) in a 640 neutron group format spanning an energy range from thermal to 20.0 MeV. Prior to use in the least squares adjustment, this fine group library is collapsed to a broad group structure consisting of 53 groups using the calculated neutron spectrum at the measurement location as a weighting function. The data comparisons from the standard field irradiations were used to determine the level of accuracy of the base cross-section library, as well as to demonstrate the adequacy of the collapsing procedure used to generate the 53 group library.

In ASTM E261-98, "Standard Practice for Determining Neutron Fluence, Fluence Rate, and Spectra by Radioactivation Techniques,"[19] fission spectrum averaged cross-sections applicable to the ^{235}U thermal fission field and the ^{252}Cf spontaneous fission field are provided for a variety

of threshold activation detectors that are used in power and research reactor irradiations. In this data compilation, both calculated and measured spectrum averaged cross-sections are provided along with their evaluated uncertainties. The magnitude of errors in the processed dosimetry cross-section library can be judged by the observed disagreement between the calculated spectrum averaged cross-sections and the corresponding measured values for the standard ^{235}U and ^{252}Cf fields.

The data listed in Tables 3-1 and 3-2 have been extracted from Table 3 of ASTM E261 and are representative of the foil sets used in power reactor irradiations and in the PCA benchmark irradiations. This subset of the ASTM E261 information includes all of the threshold reactions typically used in Light Water Reactor (LWR) surveillance capsule and ex-vessel dosimetry irradiations.

For the comparisons shown in Tables 3-1 and 3-2, the authors of ASTM E261 based the calculated spectrum averaged reaction cross-sections on data from the recommended SNLRML library. Since the Westinghouse methodology and the evaluations provided in ASTM E261-98 are both based on the same dosimetry cross-section library, the calculated spectrum averaged cross-sections produced by the SAND/FERRET processing procedure should closely match the calculated values cited in the standard. Significant differences between the two sets of calculated spectrum averaged cross-sections would indicate errors in the processing procedure. Comparisons of the calculated spectrum averaged cross-sections from ASTM E261 with the corresponding cross-sections processed by Westinghouse are listed in Table 3-3.

The calculation to measurement comparisons given in Table 3-1 indicate that for the ^{235}U thermal fission field, all of the C/M ratios except $^{46}Ti(n,p)^{46}Sc$ fall within one standard deviation of the combined uncertainty in the calculation and measurement. For these reactions, the agreement between calculation and measurement is within 5%. In the case of the $^{46}Ti(n,p)^{46}Sc$ reaction, the C/M ratio falls within two standard deviations of the combined uncertainty with the calculation falling within 11% of the measured value.

In the case of the ^{252}Cf spontaneous fission field, the comparisons provided in Table 3-2 show that, with the exception of the, $^{238}U(n,f)FP$, $^{115}In(n,n')^{115m}$, and $^{46}Ti(n,p)^{46}Sc$ reactions, all of the C/M comparisons fall within one standard deviation of the combined uncertainty in the calculations and measurements. The C/M ratios for the $^{238}U(n,f)FP$, $^{115}In(n,n')^{115m}$ reactions fall within two standard deviations and the C/M ratio for the $^{46}Ti(n,p)^{46}Sc$ reaction falls within three standard deviations of the combined uncertainty. For all reactions other than $^{46}Ti(n,p)^{46}Sc$ the agreement between calculation and measurement is within 6%. The calculated spectrum averaged cross-section for the $^{46}Ti(n,p)^{46}Sc$ reaction falls within 11% of the measured value.

The comparisons provided in Tables 3-1 and 3-2 demonstrate that the SNLRML dosimetry cross-sections as processed by the authors of ASTM E261 produce accurate representations of the spectrum averaged cross-sections in the NIST standard fission fields. The Westinghouse least squares approach uses this same base dosimetry cross-section library, but a somewhat different processing procedure.

To compare the cross-section processing procedure used in the Westinghouse approach to expand the calculated input spectrum, spectrum weight the dosimetry cross-sections, and re-collapse the spectrum and dosimetry cross-sections to the FERRET 53 energy group structure, the ASTM E261 calculations for the ^{235}U thermal fission field were duplicated for the foil reactions contained in both the power reactor sensor set and PCA sensor set. In performing this calculation, the ENDF/B-VI ^{235}U fission spectrum supplied with the BUGLE-96 cross-section library was

input to the SAND/FERRET procedure as the calculated spectrum. The dosimetry cross-sections for were taken directly from the SNLRML library.

Comparisons of the Westinghouse processed spectrum averaged cross-sections with the calculated values from ASTM E261-98 are listed in Table 3-3 for both the power reactor and PCA sensor sets. An examination of the data given in Table 3-3 shows that the spectrum averaged cross-sections calculated by Westinghouse using the SAND pre-processing module are essentially identical to the calculated values given in ASTM E261-98, with the largest difference being at the 1% level.

The comparison results summarized in Table 3-3 coupled with the C/M results listed in Tables 3-1 and 3-2 demonstrate that using the SNLRML dosimetry cross-section library coupled with the algorithms included in the SAND pre-processing module to produce a spectrum weighted broad group library, results in an appropriate cross-section representation for use in the FERRET least squares adjustment algorithm.

Table 3-1

^{235}U Fission Spectrum Averaged Cross-Sections from ASTM E261-98

Typical Power Reactor Sensor Sets			
	Spectrum Average Cross-Section (millibarns)		
Reaction	Calculation	Measurement	C/M
$^{63}Cu(n,\alpha)^{60}Co$	0.521 (2.85%, 6.05%)	0.50 (11.0%)	1.042 (12.87%)
$^{46}Ti(n,p)^{46}Sc$	10.43 (2.46%, 5.4%)	11.6 (3.45%)	0.899 (6.86%)
$^{54}Fe(n,p)^{54}Mn$	80.18 (2.17%, 4.69%)	80.5 (2.86%)	0.996 (5.91%)
$^{58}Ni(n,p)^{58}Co$	105.69 (2.43%, 4.52%)	108.5 (5.0%)	0.974 (7.16%)
$^{238}U(n,f)FP$	306.23 (0.53%, 4.21%)	309.0 (2.6%)	0.991 (4.98%)
$^{237}Np(n,f)FP$	1330.1 (9.33%, 4.31%)	1344.0 (4.0%)	0.990 (11.0%)

PCA Sensor Sets			
	Spectrum Average Cross-Section (millibarns)		
Reaction	Calculation	Measurement	C/M
$^{27}Al(n,\alpha)^{24}Na$	0.727 (1.40%, 6.95%)	0.706 (3.97%)	1.030 (8.13%)
$^{58}Ni(n,p)^{58}Co$	105.69 (2.43%, 4.52%)	108.5 (5.0%)	0.974 (7.16%)
$^{115}In(n,n')^{115m}In$	186.35 (2.17%, 4.17%)	190.3 (3.84%)	0.979 (6.07%)
$^{103}Rh(n,n')^{103m}Rh$	706.02 (3.1%, 4.14%)	733.0 (5.2%)	0.963 (7.33%)
$^{238}U(n,f)FP$	306.23 (0.53%, 4.21%)	309.0 (2.6%)	0.991 (4.98%)
$^{237}Np(n,f)FP$	1330.1 (9.33%, 4.31%)	1344.0 (4.0%)	0.990 (11.0%)

Notes: 1 - The tabulated data were taken from Table 3 of ASTM E261-98.

2 - For the calculated values, the cross-section and spectrum components of the uncertainty, respectively, are shown in parentheses.

3 - The measurement uncertainty is also shown in parentheses.

4 - The uncertainty in the C/M ratio represents a sum in quadrature of the measurement and calculational uncertainty.

Table 3-2

^{252}Cf Fission Spectrum Averaged Cross-Sections from ASTM E261-98

Typical Power Reactor Sensor Sets			
	Spectrum Average Cross-Section (millibarns)		
Reaction	Calculation	Measurement	C/M
^{63}Cu(n,α)^{60}Co	0.678 (2.83%, 1.38%)	0.689 (1.98%)	0.984 (3.72%)
^{46}Ti(n,p)^{46}Sc	12.56 (2.45%, 1.18%)	14.09 (1.76%)	0.891 (3.24%)
^{54}Fe(n,p)^{54}Mn	88.12 (2.14%, 0.79%)	86.92 (1.34%)	1.014 (2.65%)
^{58}Ni(n,p)^{58}Co	115.31 (2.40%, 0.73%)	117.6 (1.3%)	0.981 (2.83%)
^{238}U(n,f)FP	315.39 (0.53%, 0.4%)	325.0 (1.63%)	0.970 (1.76%)
^{237}Np(n,f)FP	1335.0 (9.2%, 0.23%)	1361.0 (1.58%)	0.981 (9.43%)

PCA Sensor Sets			
	Spectrum Average Cross-Section (millibarns)		
Reaction	Calculation	Measurement	C/M
^{27}Al(n,α)^{24}Na	1.04 (1.36%, 1.61%)	1.017 (1.47%)	1.019 (2.57%)
^{58}Ni(n,p)^{58}Co	115.31 (2.40%, 0.73%)	117.6 (1.3%)	0.981 (2.83%)
^{115}In(n,n')^{115m}In	189.8 (2.16%, 0.38%)	197.6 (1.3%)	0.961 (2.55%)
^{103}Rh(n,n')^{103m}Rh	714.45 (3.08%, 0.27%)	757.0 (4.0%)	0.944 (5.06%)
^{238}U(n,f)FP	315.39 (0.53%, 0.4%)	325.0 (1.63%)	0.970 (1.76%)
^{237}Np(n,f)FP	1335.0 (9.2%, 0.23%)	1361.0 (1.58%)	0.981 (9.43%)

Notes: 1 - The tabulated data were taken from Table 3 of ASTM E261-98.

2 - For the calculated values, the cross-section and spectrum components of the uncertainty, respectively, are shown in parentheses.

3 - The measurement uncertainty is also shown in parentheses.

4 - The uncertainty in the C/M ratio represents a sum in quadrature of the measurement and calculational uncertainty.

Table 3-3

Comparison of Calculated ^{235}U Fission Spectrum Averaged Cross-Sections

Typical Power Reactor Sensor Sets			
	Spectrum Average Cross-Section (millibarns)		Ratio
Reaction	ASTM E261-98	SAND/FERRET	FERRET/E261
$^{63}Cu(n,\alpha)^{60}Co$	0.521	0.523	1.004
$^{46}Ti(n,p)^{46}Sc$	10.4	10.3	0.990
$^{54}Fe(n,p)^{54}Mn$	80.2	80.3	1.001
$^{58}Ni(n,p)^{58}Co$	106	106	1.000
$^{238}U(n,f)FP$	306	306	1.000
$^{237}Np(n,f)FP$	1330	1330	1.000

PCA Sensor Sets			
	Spectrum Average Cross-Section (millibarns)		Ratio
Reaction	ASTM E261-98	SAND/FERRET	FERRET/E261
$^{27}Al(n,\alpha)^{24}Na$	0.727	0.729	1.003
$^{58}Ni(n,p)^{58}Co$	106	106	1.000
$^{115}In(n,n')^{115m}In$	186	186	1.000
$^{103}Rh(n,n')^{103m}Rh$	706	706	1.000
$^{238}U(n,f)FP$	306	306	1.000
$^{237}Np(n,f)FP$	1330	1330	1.000

3.2 EVALUATION OF THE PCA SIMULATOR BENCHMARK

The guidance provided in Regulatory Guide 1.190[3] recommends using measured data from the Pool Critical Assembly (PCA) pressure vessel simulator[13, 20, 21] to benchmark neutron transport calculational methods for application to LWR pressure vessel fluence determination. The documentation describing the PCA experimental program and the subsequent evaluation of the dosimetry data obtained from the simulator irradiations also affords the opportunity to compare the results from the Westinghouse least squares methodology using the FERRET code with similar analyses completed by other laboratories. These comparisons are valuable in that they highlight any differences that may occur due to the use of different input or different least squares adjustment codes.

In Reference 20, several least squares evaluations of dosimetry data from the PCA 12/13 configuration were documented. These evaluations were completed by Rolls Royce and Associates (RR&A), Hanford Engineering Development Laboratory (HEDL), and Oak Ridge National Laboratory (ORNL), each using a different least squares adjustment code. The results of these least squares analyses were used to establish recommended values of key neutron exposure parameters (ϕ(E > 1.0 MeV) and dpa) for this blind test configuration.

A plan view of the PCA reactor and pressure vessel simulator showing materials characteristic of the core axial midplane is shown in Figure 3-1. The configuration shown in Figure 3-1 was developed from dimensional information provided in Reference 13 and reflects the latest available geometric data for the simulator. During the PCA experiments, measurements were taken at several locations within the mockup to provide traverse data extending from the reactor core outward through the pressure vessel simulator and on into the void box. The specific measurement locations are illustrated on Figure 3-1 and listed in Table 3-4. All of the measurements of interest were obtained on the lateral centerline of the mockup at an elevation opposite the axial midplane of the simulator.

The measurement locations specified in Table 3-4 provide data sufficient to generate calculation/measurement comparisons throughout the entire 12/13 configuration. The data afford the opportunity for comparisons over a wide attenuation range with a changing neutron energy spectrum within the carbon steel simulator wall. Thus, this simulator benchmark experiment provides an excellent test for the evaluation of transport calculation and dosimetry evaluation methodologies for both in-vessel and ex-vessel irradiations.

The least squares evaluations documented in Reference 20 included data from a subset of the measurement points listed in Table 3-4. In particular, least squares comparisons were provided at locations A2, A4, A5, A6, and A7. These data locations were intended to simulate an in-vessel surveillance capsule mounted on the outer diameter of the thermal shield, the 1/4T, 1/2T, and 3/4T locations interior to the pressure vessel wall, and an ex-vessel dosimetry location in the reactor cavity external to the pressure vessel wall.

The Reference 20 analyses were completed using three different least squares adjustment codes (SENSAK[22], FERRET[5], and LSL-M2[9]). The calculated input spectra for the SENSAK analysis were based on discrete ordinates calculations using the EUROLIB-4 cross-section library. The FERRET and LSL-M2 analyses likewise used calculated spectra from discrete ordinates calculations, but based on the use of the ENDF/B-IV SAILOR cross-section library. All of these least squares evaluations used the recommended measurement data from the PCA irradiations and dosimetry reaction cross-sections from the ENDF/B-V data files.

The least squares results provided in Section 7.1 of Reference 20 are reproduced in Table 3-5. The data included in Table 3-5 show that, in terms of adjusted neutron flux (E > 1.0 MeV), the RR&A and HEDL analyses produce essentially identical results while the ORNL evaluation yields adjusted results that are lower by 4.0-8.5 percent. However, all of the reported results are consistent within the combined uncertainties quoted for the adjusted results. Thus, these prior least squares evaluations of the PCA benchmark data did not indicate any significant differences in the adjustments produced by these three codes.

As a test of the current Westinghouse least squares methodology using the FERRET code, these PCA evaluations were repeated using updated input based on the now available ENDF/B-VI neutron transport and dosimetry reaction cross-section libraries. The intent of this updated evaluation was to test the capabilities of the FERRET code as applied by Westinghouse using current methodology and data libraries.

Due to the relative small size of the PCA configuration, calculations using the typical 3D synthesis approach tend to break down at locations toward the back side of the simulator (A6, A7). Therefore, the spectrum input to the least squares analysis was taken from a fully three-dimensional calculation using the TORT code[10] run in X,Y,Z geometry. The TORT calculations were run using the BUGLE-96 cross-section library[11] with a P_3 scattering cross-section expansion and an S_8 angular quadrature. The uncertainty associated with the calculated spectrum was based on the formulation described in Section 2.3 of this report. The measured reaction rates used in the least squares evaluation of dosimetry sets from locations A1 through A7 within the PCA 12/13 configuration were the recommended values from Reference 20. The reaction rate uncertainties used in the analysis were 5% and 10% for the non-fission and fission sensors, respectively. The dosimetry reaction cross-sections and cross-section uncertainty data were obtained from the SNLRML library.[23]

Results of the FERRET least squares evaluations of the PCA dosimetry from locations A1 through A7 are given Tables 3-6 through 3-9. In Table 3-6, comparisons of the measurement to calculation ratios for each sensor are listed before and after application of the least squares procedure. The comparisons before adjustment (M/C) show that the baseline calculation and the reaction rate measurements are in good agreement for all reactions at all measurement locations with the M/C values falling in a range of 0.91-1.05. The linear average of the M/C data at each measurement location ranges from 0.97-1.02, with the standard deviations in these averages varying from 2.0-4.8%. All of these M/C comparisons fall within the 15% standard deviation ascribed to the unadjusted calculation. In aggregate, these comparisons indicate reasonable consistency between the calculated and measured reaction rates and imply that any adjustments to the calculated spectra should be relatively small.

The comparisons after adjustment (M/A) show that the adjustments are indeed small, but do result in improved agreement between the calculated and measured data. After adjustment, the M/A data for the individual sensors fall in the range of 0.94 to 1.06, while the linear average of the M/A ratios at each measurement location ranges from 0.99-1.01. The standard deviations in these linear averages have been reduced, ranging from 1.0-3.6%.

In Table 3-7, the neutron flux (E > 1.0 MeV) at each measurement location is provided before and after adjustment. The data in Table 3-7 show that the net adjustment in the fast neutron flux was 3% or less, depending on location and that the inclusion of the measurement information has reduced the uncertainty in the magnitude of the fast flux from 15% to 4%. This improved uncertainty in the fast neutron flux is consistent with the corresponding improvement in the calculated sensor reaction rates.

Detailed comparisons of the data adjustments for each measurement location are given in Table 3-8. These comparisons show that in all cases, the adjustments performed by the FERRET analysis are small and consistent with the input uncertainty bounds for the reaction rates and calculated neutron flux. The χ^2 per degree of freedom associated with each of the analyses indicate good data consistency for all cases.

Finally, in Table 3-9, the results of the current FERRET evaluation of the PCA data are compared with the prior analysis listed in Table 3-5. The newer FERRET results are essentially identical to the previous results reported by RR&A and HEDL, but with an improved uncertainty. The improvement in the uncertainty is attributable to greater accuracy in the input calculated spectra which were based on ENDF/B-VI transport cross-sections rather than on the ENDF/B-IV data libraries that were available at the time of the initial evaluations.

The analyses summarized in Tables 3-6 through 3-9 demonstrate that the FERRET code as applied by Westinghouse yields results consistent with those produced by other least squares adjustment codes for the PCA benchmark analyses. Further, the PCA evaluations show that the FERRET least squares analyses produced consistent results with no anomalous behavior for a wide range of neutron spectra characteristic of in-vessel and ex-vessel dosimetry locations as well as for locations interior to the carbon steel pressure vessel wall.

Figure 3-1

PCA 12/13 Configuration - X,Y Geometry

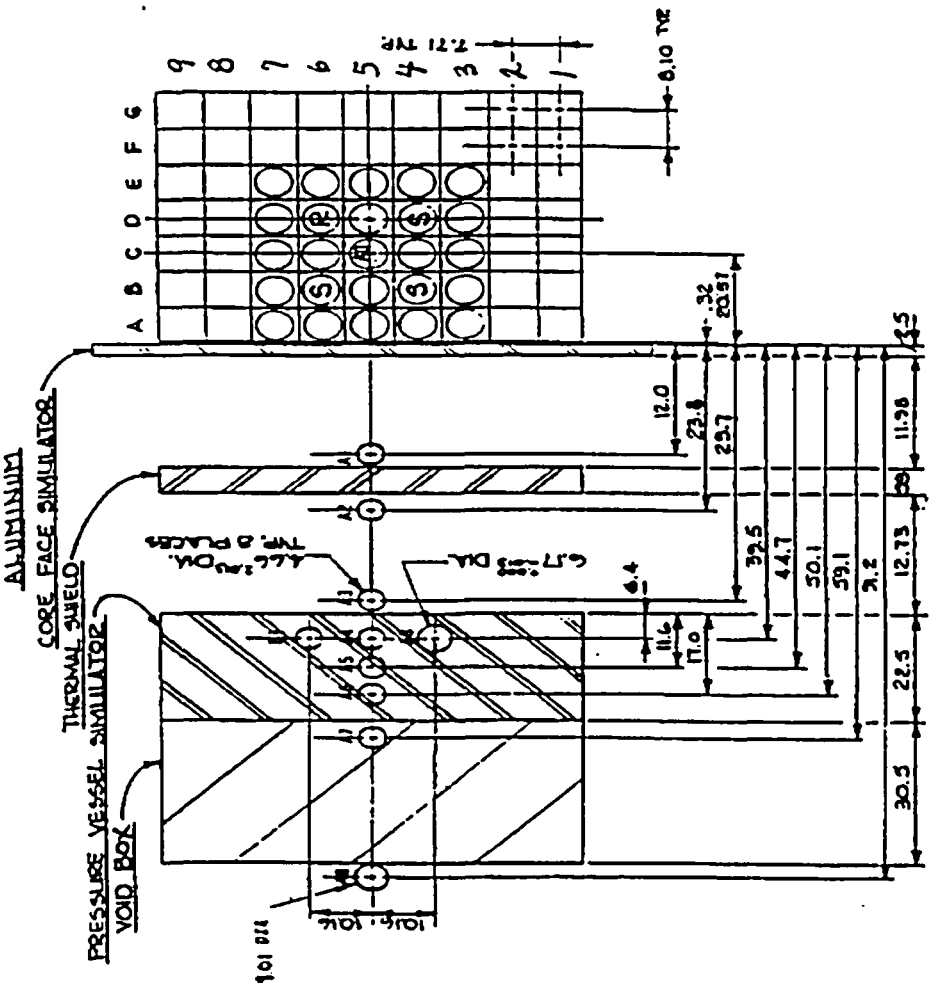

Table 3-4

Summary of Measurement Locations Within the PCA 12/13 Configuration

Measurement Location	ID	Y(cm)
Core Center	A0	-20.57
Thermal Shield Front	A1	12.0
Thermal Shield Back	A2	23.8
Pressure Vessel Front	A3	29.7
Pressure Vessel 1/4T	A4	39.5
Pressure Vessel 1/2T	A5	44.7
Pressure Vessel 3/4T	A6	50.1
Void Box	A7	59.1

Table 3-5

Least Squares Adjusted Results for the PCA 12/13 Configuration
Participating Laboratory Data from NUREG/CR-3318

Location	RR&A		HEDL		ORNL	
	$\phi(E > 1.0)$	% std.	$\phi(E > 1.0)$	% std.	$\phi(E > 1.0)$	% std.
A2	4.01e-07	9			3.85e-07	8
A4	4.50e-07	7	4.58e-08	7	4.22e-08	4
A5	2.21e-07	7	2.21e-08	7	2.03e-08	4
A6	9.73e-09	8	9.82e-09	7	8.91e-09	4
A7	2.88e-09	43				

Table 3-6

M/C Comparisons for the PCA 12/13 Blind Test Experiment

Comparisons Before Adjustment

	M/C Ratio						
	A1	A2	A3	A4	A5	A6	A7
$^{27}Al(n,\alpha)^{24}Na$ (Cd).	1.00	1.00	0.95	0.96	0.97	0.98	
$^{58}Ni(n,p)^{58}Co$ (Cd)	1.04	1.02	0.99	1.00	1.01	0.96	
$^{115}In(n,n')^{115m}In$ (Cd)	1.04	1.02	0.96	0.96	0.99	0.99	1.04
$^{103}Rh(n,n')^{103m}Rh$ (Cd)	1.01	0.97	0.97	0.96	1.02	1.05	1.05
$^{238}U(n,f)FP$ (Cd)			0.91	1.00	1.02	1.05	1.04
$^{237}Np(n,f)FP$ (Cd)			1.05	0.99	0.98	1.01	0.96
Average	1.02	1.00	0.97	0.98	1.00	1.01	1.02
% Standard Deviation	2.0	2.4	4.8	2.1	2.1	3.7	4.1

Comparisons After Adjustment

	M/A Ratio						
	A1	A2	A3	A4	A5	A6	A7
$^{27}Al(n,\alpha)^{24}Na$ (Cd)	0.99	1.01	1.01	1.01	1.01	1.00	
$^{58}Ni(n,p)^{58}Co$ (Cd)	0.99	0.99	0.98	0.98	0.99	1.02	
$^{115}In(n,n')^{115m}In$ (Cd)	0.99	0.99	1.01	1.02	1.01	1.01	1.00
$^{103}Rh(n,n')^{103m}Rh$ (Cd)	1.01	1.02	1.00	1.01	0.99	0.99	0.99
$^{238}U(n,f)FP$ (Cd)			1.06	0.98	0.98	0.94	1.00
$^{237}Np(n,f)FP$ (Cd)			0.95	1.02	1.02	1.00	1.04
Average	0.99	1.00	1.00	1.00	1.00	0.99	1.01
% Standard Deviation	1.0	1.6	3.6	1.7	1.5	2.7	2.2

Table 3-7

Summary of Least Squares Adjustment Results for the PCA 12/13 Blind Test Experiment

Location	ϕ(E > 1.0 MeV) [n/cm^2-s]		A/C
	Calculated	Adjusted	
A1	3.77e-06 (15%)	3.88e-06 (4%)	1.03
A2	4.26e-07 (15%)	4.26e-07 (4%)	1.00
A3	1.42e-07 (15%)	1.38e-07 (4%)	0.97
A4	4.73e-08 (15%)	4.62e-08 (4%)	0.98
A5	2.24e-08 (15%)	2.25e-08 (4%)	1.00
A6	9.87e-09 (15%)	9.88e-09 (4%)	1.00
A7	2.72e-09 (15%)	2.81e-09 (4%)	1.03

Note: Numbers in parentheses represent one standard deviation.

Table 3-8

FERRET Results for the PCA 12/13 Blind Test Experiment

Location A1 (χ^2/Degree of Freedom = 0.03)

Reaction	Reaction Rate [rps/atom]			Adjustment % of Calc.
	Measured	Calculated	Adjusted	
$^{27}Al(n,\alpha)^{24}Na$ (Cd Cov)	5.48e-33	5.49e-33	5.53e-33	0.7
$^{58}Ni(n,p)^{58}Co$ (Cd Cov.)	6.31e-31	6.07e-31	6.23e-31	2.6
$^{115}In(n,n')^{115m}In$ (Cd Cov.)	1.05e-30	1.01e-30	1.04e-30	3.0
$^{103}Rh(n,n')^{103m}Rh$ (CD Cov.)	4.06e-30	4.00e-30	4.10e-30	2.5
$^{238}U(n,f)FP$ (Cd Cov.)				
$^{237}Np(n,f)FP$ (Cd Cov.)				
ϕ(E >1.0 MeV) [n/cm^2-s]		3.77e-06	3.88e-06	2.9

Location A2 (χ^2/Degree of Freedom = 0.08)

Reaction	Reaction Rate [rps/atom]			Adjustment % of Calc.
	Measured	Calculated	Adjusted	
$^{27}Al(n,\alpha)^{24}Na$ (Cd Cov)	7.16e-34	7.14e-34	7.20e-34	0.8
$^{58}Ni(n,p)^{58}Co$ (Cd Cov.)	6.72e-32	6.57e-32	6.64e-32	1.1
$^{115}In(n,n')^{115m}In$ (Cd Cov.)	1.14e-31	1.12e-31	1.13e-31	0.9
$^{103}Rh(n,n')^{103m}Rh$ (CD Cov.)	4.50e-31	4.64e-31	4.60e-31	-0.9
$^{238}U(n,f)FP$ (Cd Cov.)				
$^{237}Np(n,f)FP$ (Cd Cov.)				
ϕ(E >1.0 MeV) [n/cm^2-s]		4.26e-07	4.26e-07	0.2

Location A3 (χ^2/Degree of Freedom = 0.13)

Reaction	Reaction Rate [rps/atom]			Adjustment % of Calc.
	Measured	Calculated	Adjusted	
$^{27}Al(n,\alpha)^{24}Na$ (Cd Cov)	3.13e-34	3.28e-34	3.15e-34	-4.0
$^{58}Ni(n,p)^{58}Co$ (Cd Cov.)	2.50e-32	2.53e-32	2.45e-32	-3.2
$^{115}In(n,n')^{115m}In$ (Cd Cov.)	3.68e-32	3.84e-32	3.72e-32	-3.1
$^{103}Rh(n,n')^{103m}Rh$ (CD Cov.)	1.47e-31	1.52e-31	1.47e-31	-3.3
$^{238}U(n,f)FP$ (Cd Cov.)	5.91e-12	6.47e-32	6.27e-32	-3.1
$^{237}Np(n,f)FP$ (Cd Cov.)	3.05e-31	2.90e-31	2.91e-31	0.3
ϕ(E >1.0 MeV) [n/cm^2-s]		1.42e-07	1.38e-07	-2.9

Table 3-8 (Continued)

FERRET Results for the PCA 12/13 Blind Test Experiment

Location A4 (χ^2/Degree of Freedom = 0.06)

Reaction	Reaction Rate [rps/atom]			Adjustment % of Calc.
	Measured	Calculated	Adjusted	
$^{27}Al(n,\alpha)^{24}Na$ (Cd Cov)	7.15e-35	7.46e-35	7.23e-35	-3.1
$^{58}Ni(n,p)^{58}Co$ (Cd Cov.)	5.69e-33	5.70e-33	5.58e-33	-2.1
$^{115}In(n,n')^{115m}In$ (Cd Cov.)	1.11e-32	1.15e-32	1.13e-32	-1.7
$^{103}Rh(n,n')^{103m}Rh$ (CD Cov.)	5.67e-32	5.89e-32	5.70e-32	-3.2
$^{238}U(n,f)FP$ (Cd Cov.)	1.79e-32	1.79e-32	1.75e-32	-2.2
$^{237}Np(n,f)FP$ (Cd Cov.)	1.20e-31	1.21e-32	1.19e-32	-1.7
ϕ(E >1.0 MeV) [n/cm^2-s]		4.73e-08	4.62e-08	-2.4

Location A5 (χ^2/Degree of Freedom = 0.04)

Reaction	Reaction Rate [rps/atom]			Adjustment % of Calc.
	Measured	Calculated	Adjusted	
$^{27}Al(n,\alpha)^{24}Na$ (Cd Cov)	2.92e-35	3.01e-35	2.94e-35	-2.3
$^{58}Ni(n,p)^{58}Co$ (Cd Cov.)	2.25e-33	2.24e-33	2.23e-33	-0.4
$^{115}In(n,n')^{115m}In$ (Cd Cov.)	5.20e-33	5.27e-33	5.27e-33	0.0
$^{103}Rh(n,n')^{103m}Rh$ (CD Cov.)	3.24e-32	3.17e-32	3.22e-32	1.6
$^{238}U(n,f)FP$ (Cd Cov.)	7.88e-33	7.70e-33	7.70e-33	0.0
$^{237}Np(n,f)FP$ (Cd Cov.)	6.56e-32	6.71e-32	6.66e-32	-0.7
ϕ(E >1.0 MeV) [n/cm^2-s]		2.24e-08	2.25e-08	0.2

Location A6 (χ^2/Degree of Freedom = 0.04)

Reaction	Reaction Rate [rps/atom]			Adjustment % of Calc.
	Measured	Calculated	Adjusted	
$^{27}Al(n,\alpha)^{24}Na$ (Cd Cov)	1.12e-35	1.15e-35	1.12e-35	-2.6
$^{58}Ni(n,p)^{58}Co$ (Cd Cov.)	7.99e-34	8.29e-34	8.14e-34	-1.8
$^{115}In(n,n')^{115m}In$ (Cd Cov.)	2.23e-33	2.26e-33	2.25e-33	-0.4
$^{103}Rh(n,n')^{103m}Rh$ (CD Cov.)	1.67e-32	1.60e-32	1.66e-32	3.7
$^{238}U(n,f)FP$ (Cd Cov.)	3.26e-33	3.09e-33	3.07e-33	-0.6
$^{237}Np(n,f)FP$ (Cd Cov.)	3.46e-32	3.43e-32	3.47e-32	1.2
ϕ(E >1.0 MeV) [n/cm^2-s]		9.87e-09	9.88e-09	0.1

Table 3-8 (Continued)

FERRET Results for the PCA 12/13 Blind Test Experiment

Location A7(χ^2/Degree of Freedom = 0.04

Reaction	Reaction Rate [rps/atom]			Adjustment % of Calc.
	Measured	Calculated	Adjusted	
$^{27}Al(n,\alpha)^{24}Na$ (Cd Cov)				
$^{58}Ni(n,p)^{58}Co$ (Cd Cov.)				
$^{115}In(n,n')^{115m}In$ (Cd Cov.)	6.43e-34	6.20e-34	6.40e-34	3.2
$^{103}Rh(n,n')^{103m}Rh$ (CD Cov.)	4.83e-33	4.60e-33	4.80e-33	4.3
$^{238}U(n,f)FP$ (Cd Cov.)	8.65e-34	8.33e-34	8.61e-34	3.4
$^{237}Np(n,f)FP$ (Cd Cov.)	9.60e-33	9.97e-33	9.98e-33	0.1
ϕ(E >1.0 MeV) [n/cm^2-s]		2.72e-09	2.81e-09	3.2

Table 3-9

Comparison of Current FERRET Least Squares Results with Prior Analyses
PCA 12/13 Configuration

	FERRET		RR&A		HEDL		ORNL	
	ϕ(E>1.0)	% std.	ϕ(E>1.0)	% std.	ϕ(E>1.0)	% std.	ϕ(E>1.0)	% std.
A1	3.88e-06	4						
A2	4.26e-07	4	4.01e-07	9			3.85e-07	8
A3	1.38e-07	4						
A4	4.62e-08	4	4.50e-07	7	4.58e-08	7	4.22e-08	4
A5	2.25e-08	4	2.21e-07	7	2.21e-08	7	2.03e-08	4
A6	9.88e-09	4	9.73e-09	8	9.82e-09	7	8.91e-09	4
A7	2.81e-09	4	2.88e-09	43				

3.3 EVALUATION OF THE H. B. ROBINSON BENCHMARK

In performing the benchmarking of the neutron transport methodology described in Section 2.3 of this report, comparisons of calculations using ENDF/B-VI cross-sections with measured reaction rates from both in-vessel and ex-vessel dosimetry sets irradiated in the H. B. Robinson Cycle 9 benchmark experiment were used. This direct comparison of the calculated reaction rates with measurements showed excellent agreement. As a further demonstration of the application of the least squares procedure using the FERRET code, an evaluation of the in-vessel and ex-vessel data from the H. B. Robinson benchmark was also completed.

The neutron transport calculations input to the least squares analysis were completed using the standard synthesis approach described in Section 2.3 of this report. The calculations were run using the BUGLE-96 cross-section library[11] with a P_3 scattering cross-section expansion and an S_8 angular quadrature. The uncertainty associated with the calculated spectrum was likewise based on the formulation described in Section 2.3 of this report. The measured reaction rates used in the least squares evaluation of the dosimetry were the recommended values from Reference 25. The reaction rate uncertainties used in the analysis were 5% and 10% for the non-fission and fission sensors, respectively. The dosimetry reaction cross-sections and cross-section uncertainty data were obtained from the SNLRML library.[23]

Results of the least squares evaluation of the H. B. Robinson in-vessel and ex-vessel sensor sets are provided in Tables 3-10 through 3-12. Detailed comparisons of the data adjustments for each measurement location are given in Table 3-10. These comparisons show that in both cases the adjustments performed by the FERRET analysis are small and consistent with the input uncertainty bounds for the reaction rates and calculated neutron flux. The χ^2 per degree of freedom associated with each of the analyses indicate good data consistency for all cases.

In Table 3-11, the neutron flux (E > 1.0 MeV) at each measurement location is provided before and after adjustment. The data in Table 3-11 show that the net adjustment in the fast neutron flux was 1% for the in-vessel dosimetry and 2% for the ex-vessel data set. Further, the inclusion of the measurement information has reduced the uncertainty in the magnitude of the fast flux from 15% to 5% and 7% at the in-vessel and ex-vessel locations, respectively. This improved uncertainty in the fast neutron flux is consistent with the corresponding improvement in the calculated sensor reaction rates and with the FERRET analysis performed for the PCA data sets.

In Table 3-12, comparisons of the measurement to calculation ratios for each sensor are listed before and after application of the least squares procedure. The comparisons before adjustment (M/C) show that the baseline calculation and the reaction rate measurements are in good agreement for all reactions at all measurement locations with the M/C values falling in a range of 0.95-1.11. The linear average of the M/C data at both measurement locations is 1.03, with the standard deviations in these averages being 4.4 and 5.2% for the in-vessel and ex-vessel data, respectively. All of these M/C comparisons fall within the 15% standard deviation ascribed to the unadjusted calculation. In aggregate, these comparisons indicate reasonable consistency between the calculated and measured reaction rates and imply that any adjustments to the calculated spectra should be relatively small.

The comparisons after adjustment (M/A) show that the adjustments are indeed small, but do result in improved agreement between the calculated and measured data. After adjustment the M/A data for the individual sensors is improved and falls in the range of 0.96 to 1.09 while the linear average of the M/A ratios at both measurement location is 1.01. The standard deviations in

these linear averages have been reduced, ranging from 3.6% at the in-vessel location to 5.0% in the reactor cavity.

The comparisons summarized in Tables 3-10 through 3-12 support the analyses previously presented for the PCA benchmark experiment and further demonstrate the applicability of the FERRET code and the least squares procedure used by Westinghouse for analysis of LWR dosimetry data.

Table 3-10

FERRET Results for the H. B. Robinson Benchmark Experiment

In-Vessel (χ^2/Degree of Freedom = 0.23)

Reaction	Reaction Rate [rps/atom]			Adjustment % of Calc.
	Measured	Calculated	Adjusted	
$^{63}Cu(n,\alpha)^{60}Co$	3.98e-17	3.85e-17	3.97e-17	3.1
$^{46}Ti(n,p)^{46}Sc$	6.49e-16	6.07e-16	6.30e-16	3.8
$^{54}Fe(n,p)^{54}Mn$	3.83e-15	3.79e-15	3.84e-15	1.3
$^{58}Ni(n,p)^{58}Co$	4.88e-15	5.13e-15	5.10e-15	-0.6
$^{238}U(n,p)FP$	1.80e-14	1.68e-14	1.69e-14	0.6
$^{237}Np(n,p)FP$	1.20e-13	1.18e-13	1.18e-13	0.0
ϕ(E >1.0 MeV) [n/cm^2-s]		4.60e+10	4.57e+10	-0.7

Ex-Vessel (χ^2/Degree of Freedom = 0.44)

Reaction	Reaction Rate [rps/atom]			Adjustment % of Calc.
	Measured	Calculated	Adjusted	
$^{63}Cu(n,\alpha)^{60}Co$	4.01e-19	3.88e-19	4.09e-19	5.4
$^{46}Ti(n,p)^{46}Sc$	6.17e-18	5.54e-18	5.82e-18	5.1
$^{54}Fe(n,p)^{54}Mn$	3.59e-17	3.53e-17	3.67e-17	4.0
$^{58}Ni(n,p)^{58}Co$	5.29e-17	5.32e-17	5.49e-17	3.2
$^{238}U(n,p)FP$	2.72e-16	2.44e-16	2.50e-16	2.5
ϕ(E >1.0 MeV) [n/cm^2-s]		9.65e+08	9.80e+08	1.6

Table 3-11

Summary of Least Squares Adjustment Results for the H. B. Robinson Benchmark

Location	ϕ(E > 1.0 MeV) [n/cm^2-s]		A/C
	Calculated	Adjusted	
In-Vessel	4.60e+10 (15%)	4.57e+10 (5%)	0.99
Ex-Vessel	9.65e+08 (15%)	9.80e+08 (7%)	1.02

Note: Numbers in parentheses represent one standard deviation.

Table 3-12

M/C Comparisons for the H. B. Robinson Benchmark

Comparisons Before Adjustment

Reaction	M/C	
	In-Vessel	Ex-Vessel
$^{63}Cu(n,\alpha)^{60}Co$	1.03	1.03
$^{46}Ti(n,p)^{46}Sc$	1.07	1.11
$^{54}Fe(n,p)^{54}Mn$	1.01	1.02
$^{58}Ni(n,p)^{58}Co$	0.95	0.99
$^{238}U(n,p)FP$	1.07	1.11
$^{237}Np(n,p)FP$	1.02	
Average	1.03	1.03
% Standard Deviation	4.4	6.5

Comparisons After Adjustment

Reaction	M/C	
	In-Vessel	Ex-Vessel
$^{63}Cu(n,\alpha)^{60}Co$	1.00	0.98
$^{46}Ti(n,p)^{46}Sc$	1.03	1.06
$^{54}Fe(n,p)^{54}Mn$	1.00	0.98
$^{58}Ni(n,p)^{58}Co$	0.96	0.96
$^{238}U(n,p)FP$	1.07	1.09
$^{237}Np(n,p)FP$	1.02	
Average	1.01	1.01
% Standard Deviation	3.6	5.0

4.0 FERRET SENSITIVITY STUDIES

The information discussed in this section is intended to provide an understanding of how the composition of the multiple foil sensor sets and the input values for the uncertainties in the calculated neutron spectrum and measured reaction rates impact the results of the least squares analysis in terms of both the magnitude and uncertainty of the best estimate spectrum.

The threshold foils comprising typical LWR sensor sets respond to different portions of the neutron energy spectrum. This response is highlighted in Figures 4-1 and 4-2 for the neutron spectra characteristic of an in-vessel surveillance capsule location and an ex-vessel dosimetry location. The graphical representations shown in Figures 4-1 and 4-2 provide response profiles for the $^{63}Cu(n,\alpha)$, $^{54}Fe(n,p)$, $^{238}U(n,f)$, and $^{237}Np(n,f)$ threshold reactions, as well as for the neutron flux (E > 1.0 MeV). The $^{46}Ti(n,p)$ and $^{58}Ni(n,p)$ reactions exhibit behavior similar to the $^{63}Cu(n,\alpha)$, $^{54}Fe(n,p)$ reactions, respectively.

From Figures 4.1 and 4.2, it is evident that the response of the higher threshold reactions exhibits significantly different behavior than does the neutron flux (E > 1.0 MeV), while the fission monitor response shows a better match to the spectral behavior of the neutron flux. This behavior suggests that in order to validate a calculation of the neutron flux (E > 1.0 MeV), significant spectral weighting of measured reaction rates should be included in the comparisons. The least squares approach allows this spectral weighting to be included in a rigorous manner. The data from Figures 4-1 and 4-2 also indicate that the makeup of the foil set could have an impact on the final results of the dosimetry comparisons.

4.1 COMPOSITION OF THE MULTIPLE FOIL SENSOR SET

In order to assess the impact of the makeup of the sensor set on the final solution of the least squares adjustment, a parametric study was performed for a typical LWR dosimetry data set. In the parametric study, the calculated neutron spectrum and uncertainty was held constant along with the uncertainties associated with the measured reaction rates. The base case consisted of an evaluation including all of the threshold reactions while the variations in the analysis were accomplished by deleting foil reactions individually and in combination. The 11 cases analyzed in the parametric study are summarized as follows:

	Foils Included in the FERRET Analysis					
Case	Cu	Ti	Fe	Ni	^{238}U	^{237}Np
1	X	X	X	X	X	X
2	X		X	X	X	X
3	X		X		X	X
4			X		X	X
5			X			X
6			X		X	
7					X	X
8						X
9					X	
10			X			
11	X					

The results of the least squares evaluations for each of these 11 cases are as follows:

Case	ϕ(E > 1.0 MeV) [n/cm^2-s]		A/C	% Diff From Case 1
	Calculated	Adjusted		
1	4.45e+10 (15%)	4.64e+10 (6%)	1.04	
2	4.45e+10 (15%)	4.64e+10 (6%)	1.04	0.0
3	4.45e+10 (15%)	4.75e+10 (6%)	1.07	2.4
4	4.45e+10 (15%)	4.76e+10 (6%)	1.07	2.6
5	4.45e+10 (15%)	4.69e+10 (7%)	1.05	1.1
6	4.45e+10 (15%)	4.78e+10 (7%)	1.07	3.0
7	4.45e+10 (15%)	4.79e+10 (8%)	1.08	3.2
8	4.45e+10 (15%)	4.60e+10 (12%)	1.03	-0.9
9	4.45e+10 (15%)	4.84e+10 (9%)	1.09	4.3
10	4.45e+10 (15%)	4.69e+10 (9%)	1.05	1.1
11	4.45e+10 (15%)	4.80e+10 (12%)	1.08	3.4

Note: Numbers in parentheses represent one standard deviation.

This data tabulation shows that in terms of the magnitude of the adjusted solution the results for all cases are within the uncertainty of the base case (Case 1). However, the uncertainty in the adjusted flux increases as the content of the foil set is reduced with the highest uncertainties occurring when only a single foil is used in conjunction with the transport calculation.

The data in the tabulation further shows that for a minimum uncertainty solution the foil set should consist of at least Fe, U, and Np foils (Case 4). The addition of Cu, Ti, and Ni do not enhance the capability of the foil set. This is due to the fact that the very high threshold of the ^{63}Cu(n, α) and ^{46}Ti(n,p) reactions places their response well above the important energy range for the neutron flux (E > 1.0 MeV) and the ^{58}Ni(n,p) response is so similar to ^{54}Fe(n,p) that the reaction is redundant. Further reductions in the foil set from the Fe, ^{238}U, ^{237}Np package results in an increased uncertainty in the adjusted flux.

4.2 INPUT UNCERTAINTIES

A second sensitivity study was completed to evaluate the impact of the input uncertainties in the measured reaction rates and the calculated neutron flux on the adjusted solution and the final uncertainties determined by the FERRET least squares procedure. In performing this sensitivity study, the following uncertainty matrix was evaluated for the reaction rates and calculated spectra:

Reaction Rate Uncertainties

Reaction Type	Uncertainty Category		
	High	Medium	Low
Non-Fission	10%	5%	2.5%
Fission	20%	10%	5.0%

Neutron Spectrum Uncertainties

Reaction Type	Uncertainty Category		
	High	Medium	Low
Normalization	30%	20%	10%
Spectrum Groups 1-53	30%	20%	10%
Spectrum Groups 28-48	50%	25%	10%
Spectrum Groups 48-53	100%	50%	25%

In this sensitivity study, the "High" category would tend to overstate achievable uncertainties, the "Medium" category would represent a routinely achievable case, and the "low" category would be equivalent to values achievable in the laboratory or benchmark environment.

The results of the input uncertainty sensitivity study are summarized as follows:

Adjusted $\phi(E > 1.0\ MeV)$ and % Standard Deviation

Flux Spectrum Uncertainty	Reaction Rate Uncertainty		
	High	Medium	Low
High	2.05e+10 (16%)	2.11e+10 (14%)	2.14e+10 (13%)
Medium	1.99e+10 (12%)	2.04e+10 (10%)	2.10e+10 (9%)
Low	2.00e+10 (7%)	1.98e+10 (6%)	2.03e+10 (5%)

Considering the "Medium"-"Medium" case as the baseline, the magnitude of the adjusted flux varies by less than 5% for all of the cases evaluated, indicating that the magnitude of the adjusted flux is dependent primarily on the magnitude of the inputs, rather than on the input uncertainties. However, the associated uncertainty varies in a predictable trend from 5% for the "Low"-"Low" case to 16% for the "High"-"High".

The indications from this sensitivity study indicate that the FERRET least squares algorithm is operating as anticipated.

Figure 4-1

Cumulative Sensor Response as a Function of Neutron Energy
In-Vessel Surveillance Capsule Location

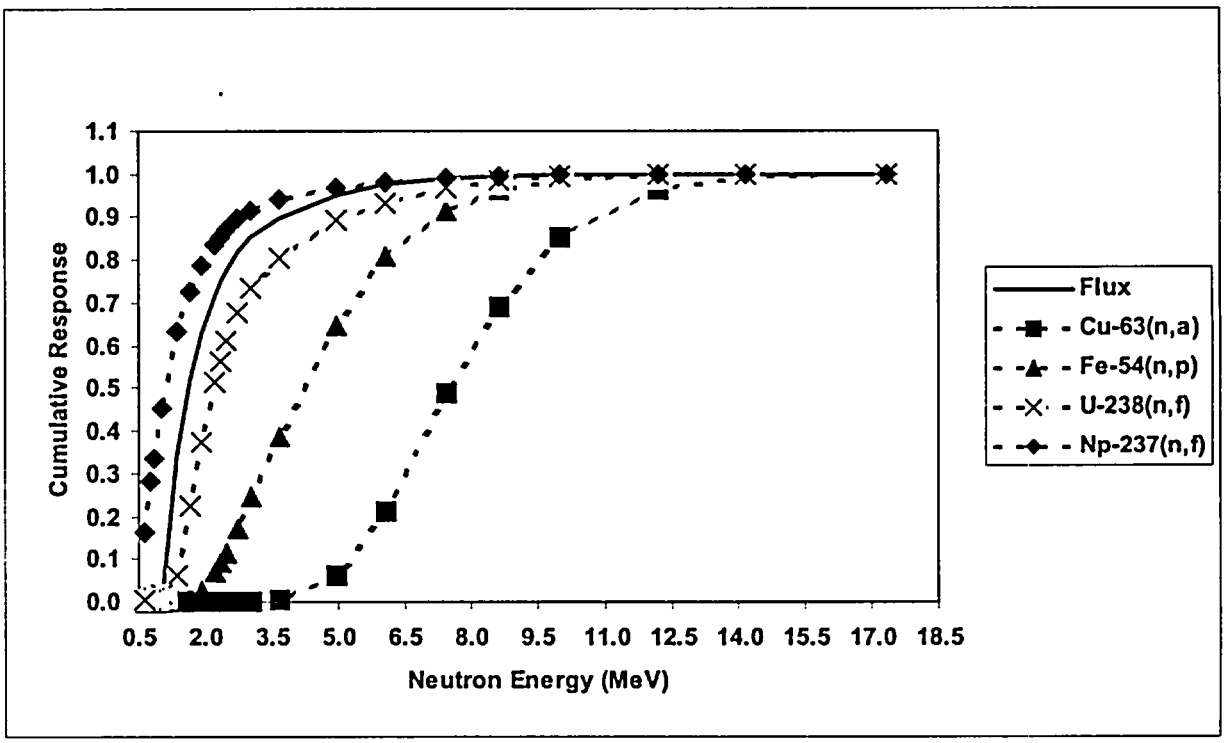

Figure 4-2

Cumulative Sensor Response as a Function of Neutron Energy
Ex-Vessel Dosimetry Location

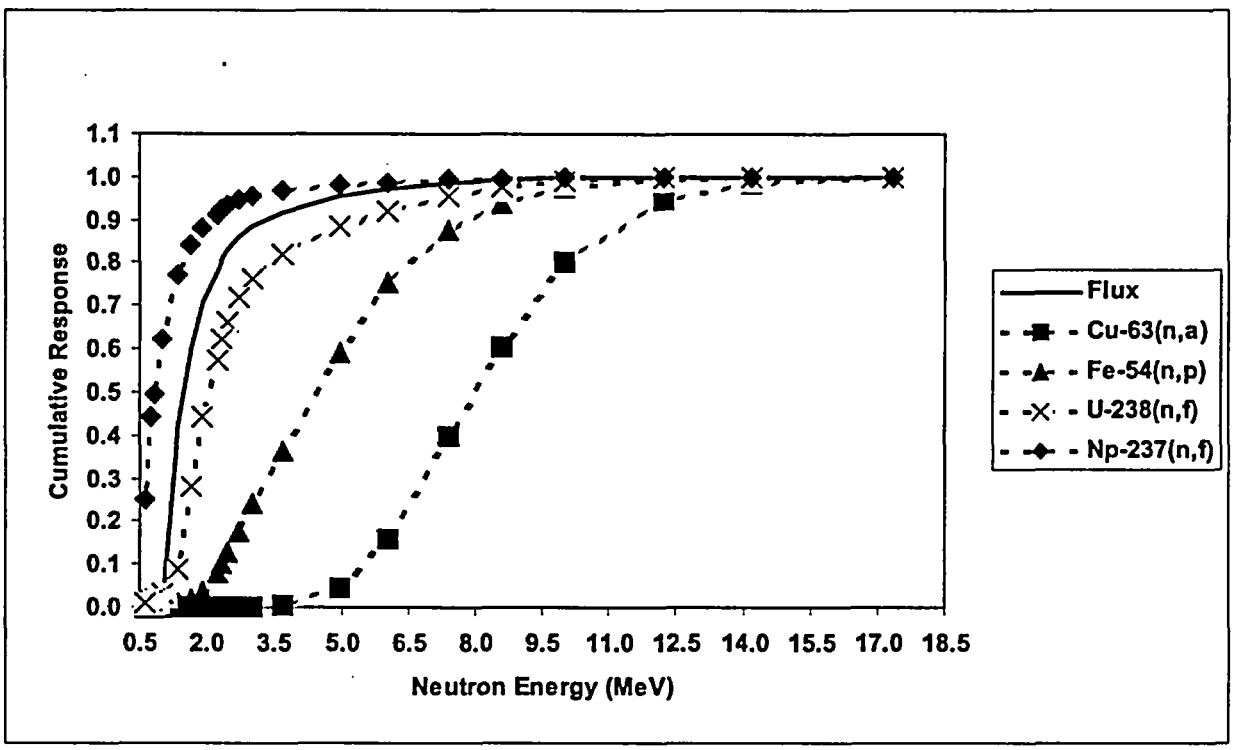

5.0 SUMMARY AND CONCLUSIONS

In this report, the use of the FERRET adjustment code for the least squares evaluation of LWR surveillance dosimetry has been described and benchmarked. The ability of the least squares procedure to combine calculations with available measurements to determine the best estimate spectrum with reduced uncertainties at the measurement locations has been demonstrated by benchmark comparisons in the NIST ^{235}U and ^{237}Np standard fission fields, the PCA simulator benchmark, and the H. B. Robinson power reactor benchmark.

The importance of the key input parameters (Neutron spectrum, measured reaction rates, and dosimetry cross-sections) and their associated uncertainties have been discussed and the values used in the Westinghouse least squares procedure have been described and justified. The sensitivity of the adjustment procedure to the makeup of the foil set and the input uncertainties in the calculated spectrum and the measured reaction rates has been provided.

The conclusions from these studies are as follows:

1 - The FERRET code operates as intended as a least squares adjustment code for reactor dosimetry analyses.

2 - The input parameters (calculated neutron spectrum, measured reaction rates, and dosimetry reaction cross-sections) and their associated uncertainties are appropriate for use in LWR dosimetry evaluations.

3 - The adjusted neutron flux (E > 1.0 MeV) from the FERRET evaluations can be used to develop a database for use in validating plant specific neutron transport calculations for LWR pressure vessels. This adjustment process provides a rigorous spectrum weighting of individual reaction rate M/C comparisons.

The comparison database developed from the least squares evaluation of the dosimetry sets can be used along with the guidance in Regulatory Guide 1.190 to validate neutron transport calculations and to determine any calculational biases that may be present.

6.0 REFERENCES

1- Code of Federal Regulations Title 10 Part 50, "Domestic Licensing of Production and Utilization Facilities," Appendix G, "Fracture Toughness Requirements" and Appendix H, "Reactor Vessel Material Surveillance Requirements,"

2- Code of Federal Regulations Title 10 Part 50.61, "Fracture Toughness Requirements for Protection Against Pressurized Thermal Shock Events,"

3- Regulatory Guide 1.190, "Calculational and Dosimetry Methods for Determining Pressure Vessel Neutron Fluence," U.S. Nuclear Regulatory Commission, Office of Nuclear Regulatory Research, March 2001.

4- ASTM Designation E944-02, "Standard Guide for Application of Neutron Spectrum Adjustment Methods in Reactor Surveillance," Annual Book of ASTM Standards, Section 12, Volume 12.02, 2003.

5- RSIC Code Package PSR-145, "FERRET Least Squares Solution to Nuclear Data and Reactor Physics Problems," Radiation Shielding Information Center, Oak Ridge National Laboratory (ORNL), January 1980.

6- F. Schmittroth, "FERRET Data Analysis Code," HEDL-TME-79-40, Hanford Engineering Development Laboratory, September 1979.

7- RSIC Code Package PSR-277, "LEPRICON PWR Pressure Vessel Surveillance Dosimetry Analysis System," Radiation Shielding Information Center, Oak Ridge National Laboratory (ORNL), June 1995.

8- RSIC Code Package PSR-113, "STAY'SL Least Squares Dosimetry Unfolding Code System," ," Radiation Shielding Information Center, Oak Ridge National Laboratory (ORNL), December 1991.

9- RSIC Code Package PSR-233, "LSL-M2 Least Squares Logarithmic Adjustment of Neutron Spectra," Radiation Shielding Information Center, Oak Ridge National Laboratory (ORNL), February 1991.

10- RSICC Computer Code Collection CCC-650, "DOORS 3.1, One- Two- and Three-Dimensional Discrete Ordinates Neutron/Photon Transport Code System," Radiation Safety Information Computational Center, Oak Ridge National Laboratory (ORNL), August 1996.

11- RSIC Data Library Collection DLC-185, "BUGLE-96, Coupled 47 Neutron, 20 Gamma Ray Group Cross-Section Library Derived from ENDF/B-VI for LWR Shielding and Pressure Vessel Dosimetry Applications," Radiation Shielding Information Center, Oak Ridge National Laboratory (ORNL), March 1996.

12- R. L. Simons, et. al, "Re-Evaluation of the Dosimetry for Reactor Pressure Vessel Surveillance Capsules," in NUREG/CP-0029, "Proceedings o the Fourth ASTM-EURATOM Symposium on Reactor Dosimetry," F. B. K. Kam, Editor, July 1982.

13- W. N. McElroy, et. al, "LWR PV Surveillance Dosimetry Improvement Program: PCA Experiments and Blind Test," NUREG/CR-1861, July 1981.

14- Regulatory Guide 1.99, Revision 2, "Radiation Embrittlement of Reactor Vessel Materials," U. S. Nuclear Regulatory Commission, Office of Nuclear Regulatory Research, May 1988.

15- G. L. Guthrie, "Uncertainty Considerations in Development and Application of Charpy Trend Curve Formulas," in REACTOR DOSIMETRY Dosimetry Methods for Fuels, Cladding, and Structural Materials, Proceedings of the Fifth ASTM-Euratom Symposium on reactor Dosimetry, GKSS Research Centre, Geesthact, F. R. G., J. P Genthon and H Rottger, Editors, D. Reidel Publishing Company, 1985.

16- G. L. Guthrie, "Charpy Trend Curve Development Based on PWR Surveillance Data," in NUREG/CP-0048 Proceedings of the U. S. nuclear Regulatory Commission Eleventh Water Reactor Safety research Information Meeting, Volume 4 – Materials Engineering Research," U. S. Nuclear Regulatory Commission, Office of Nuclear Regulatory Research, January 1984.

17- G. L. Guthrie, "Charpy Trend Curves Based on 177 PWR Data Points," NUREG/CR-3391, Volume 2, LWR-PV-SDIP Quarterly Progress Report, April 1983.

18- ASTM Designation E1018-01, "Standard Guide for Application of ASTM Evaluated Cross-Section Data File," Annual Book of ASTM Standards, Section 12, Volume 12.02, 2003.

19- ASTM Designation E261-98, "Standard Practice for Determining Neutron Fluence, Fluence Rate, and Spectra by Radioactivation Techniques," Annual Book of ASTM Standards, Section 12, Volume 12.02, 2003.

20- W. N. McElroy, et. al, "LWR Pressure Vessel Surveillance Dosimetry Improvement Program: PCA Experiments, Blind Test, and Physics-Dosimetry Support for the PSF Experiments" NUREG/CR-3318, September 1984.

21- I. Remec and F. B. K. Kam, "Pool Critical Assembly Pressure Vessel Facility Benchmark," NUREG/CR-6454, July 1997.

22- A. K. McCracken, "Few Channel Unfolding in Shielding – The SENSAK Code," in Proceedings of the 3rd ASTM-EURATOM Symposium on Reactor Dosimetry, Ispra, Italy, October 1-5, 1979, EUR 6813, Commission of the European Communities, Vol. II, P. 732, 1980.

23- RSIC Data Library Collection DLC-178, "SNLRML Recommended Dosimetry Cross Section Compendium," Radiation Shielding Information Center, Oak Ridge National Laboratory, July 1994.

24- N. P. Kocherov, et. al, "International Reactor Dosimetry File (IRDF-90)," International Atomic Energy Agency, Nuclear data Section, IAEA-NDS-141, Rev. 0, August 1990.

25- I. Remec and F. B. K. Kam, "H. B. Robinson Pressure Vessel Benchmark," NUREG/CR-6453 (ORNL/TM-13204), February 1998.

26- J. D. Andrachek, et. al, "Methodology Used to Develop Cold Overpressure Mitigating System Setpoints and RCS Heatup and Cooldown Limit Curves," WCAP-14040, Revision 3, April 2002.